Advanced Drug Delivery Reviews 177 (2021) 113847

Contents lists available at ScienceDirect

Advanced Drug Delivery Reviews

journal homepage: www.elsevier.com/locate/adr

Ultrasound and microbubbles to beat barriers in tumors: Improving delivery of nanomedicine ☆

Sofie Snipstad [a,b,c,*], Krister Vikedal [a], Matilde Maardalen [a], Anna Kurbatskaya [a], Einar Sulheim [a,b], Catharina de Lange Davies [a]

[a] Department of Physics, Norwegian University of Science and Technology, Trondheim, Norway
[b] Department of Biotechnology and Nanomedicine, SINTEF Industry, Trondheim, Norway
[c] Cancer Clinic, St. Olav's Hospital, Trondheim, Norway

ARTICLE INFO

Article history:
Received 29 April 2021
Revised 18 June 2021
Accepted 22 June 2021
Available online 25 June 2021

Keywords:
Sonopermeation
Perfusion
Extravasation
Extracellular matrix
Immune response
Nanomedicine

ABSTRACT

Successful delivery of drugs and nanomedicine to tumors requires a functional vascular network, extravasation across the capillary wall, penetration through the extracellular matrix, and cellular uptake. Nanomedicine has many merits, but penetration deep into the tumor interstitium remains a challenge. Failure of cancer treatment can be caused by insufficient delivery of the therapeutic agents. After intravenous administration, nanomedicines are often found in off-target organs and the tumor extracellular matrix close to the capillary wall. With circulating microbubbles, ultrasound exposure focused toward the tumor shows great promise in improving the delivery of therapeutic agents. In this review, we address the impact of focused ultrasound and microbubbles to overcome barriers for drug delivery such as perfusion, extravasation, and transport through the extracellular matrix. Furthermore, we discuss the induction of an immune response with ultrasound and delivery of immunotherapeutics. The review discusses mainly preclinical results and ends with a summary of ongoing clinical trials.

Contents

1. Introduction

Chemotherapy is a cornerstone in the treatment of advanced cancer and is used alone or in combination with radiotherapy or surgery. However, a major problem is that only a very small fraction of the drug is taken up by the cancer cells in solid tumors [1,2], and toxicity toward normal tissue limits the doses that can be administered. Formulating cytotoxic drugs into nanoparticles (NPs) has been a strategy to improve tumor-specific accumulation of drugs by exploiting the enhanced permeability and retention (EPR) effect [3], or as recently suggested, enhanced transcellular transport [4]. However, NPs in clinical practice have mainly improved the toxicity profile of the encapsulated cytostatic drug

☆ This review is part of the Advanced Drug Delivery Reviews theme issue on "Biological Barriers".

* Corresponding author at: Høgskoleringen 5, 7491 Trondheim, Norway.
E-mail address: sofie.snipstad@ntnu.no (S. Snipstad).

https://doi.org/10.1016/j.addr.2021.113847
0169-409X/

and have generally not improved efficacy [5]. New NP technology and clinical trials stratifying likely nanomedicine responders might improve the therapeutic response [6,7]. Still, achieving maximal therapeutic effect of small molecular drugs and nanomedicines is difficult due to the biological barriers restricting delivery to the tumor. To reach its target, the therapeutic agents depend on the vascular network and perfusion in the tumor, extravasation across the capillary wall, penetration through the extracellular matrix (ECM), and finally internalization into the cancer cells. For NPs being rather large compared to small molecular drugs, these transport barriers are even more challenging to overcome.

To improve the delivery of therapeutic agents, the administration can be combined with biological, chemical, or physical treatments. Focused ultrasound (FUS) toward the tumor is a promising approach, especially in combination with microbubbles (MBs). FUS is non-invasive, provides enhanced localized uptake of drugs and NPs in tumors, and has improved the therapeutic response both preclinically [8–14] and clinically [15,16]. A more comprehensive list of preclinical studies can be found in [17]. The combination of FUS and MBs can generate thermal or mechanical effects, depending on the frequency and acoustic pressures applied. In drug delivery, the mechanical effects are commonly exploited. The mechanical effects can be divided into acoustic radiation force and cavitation. Acoustic radiation force is caused by the loss of acoustic energy due to absorption and scattering of ultrasound (US) waves. The energy loss corresponds to a loss of momentum of the wave, which is transferred to the tissue [18–21]. This will generate a force in the direction of the US wave, which can cause acoustic streaming, shear stresses, tissue displacement, push MBs toward the blood vessel wall, and improve NP penetration through the ECM [18,21,22].

The formation, growth, and collapse of bubbles induced by US exposure are referred to as cavitation [20]. Formation of bubbles can occur when the local pressure drops to a level below the vapor pressure of the medium. This requires high acoustic pressures. Exogenous MBs are introduced to obtain oscillating MBs at lower acoustic pressures, which will expand at low local pressure and contract at high local pressure. At low acoustic pressures, these oscillations will be symmetric and mostly linear and are referred to as stable cavitation. Increasing the acoustic pressure will result in non-linear behavior of the MBs with more expansion than compression, and the MBs will be forced to oscillate until they collapse [23,24]. The oscillations of MBs result in microstreaming in the surrounding fluid and shear stress on the boundaries in the proximity of the MBs. In the case of inertial cavitation, the collapsing MBs can cause shock waves and microjets when close to a rigid boundary [21,24,25]. The threshold for inertial cavitation depends on properties of the MBs (e.g. initial size, shell type, gas) and environmental conditions [19,21,24]. The behavior of MBs and their role in drug delivery have been extensively described in two recent review articles [24,25].

To optimize FUS and MBs for drug delivery, it is essential to understand the impact their properties have on transport mechanisms. The oscillating MBs are reported to form pores (called sonoporation), open intercellular junctions, stimulate endocytosis/transcytosis, and change the (tumor) microenvironment. These processes are collectively called sonopermeation [17]. Currently, the detailed transport mechanisms are poorly understood, especially the effect of sonopermeation on perfusion and transport through the ECM. Furthermore, it is difficult to compare various studies due to the range of US parameters applied (frequency, acoustic pressure, pulse length, pulse repetition frequency, and overall exposure time) in combination with various lipid-based MBs such as SonoVue (Bracco), Sonazoid (GE Healthcare), and Definity (Lantheus), or protein-based MBs such as Optison (GE Healthcare). Additionally, multiple new MB platforms have been developed specifically for drug delivery in the last years [24–26], such as phase-shifting microdroplets or microclusters [27], nanobubbles and nanodroplets [28–31], drug-loaded MBs [32–34], targeted MBs [35] and monodisperse MBs [36,37].

The effect of US and MBs on the cellular barrier was recently extensively reviewed by Deprez et al. [38]. In this review, we address three main barriers for successful drug delivery to tumors; perfusion, extravasation, and ECM-penetration, and how sonopermeation can overcome these. Possible induction of an immune response by FUS and MBs, and combining sonopermeation and immunotherapy, are also discussed (Fig. 1).

2. Barriers for drug delivery

2.1. Changing the vasculature and perfusion

Tumor vasculature is highly heterogeneous and does not conform to the standard normal blood vessel morphology (i.e. artery – capillary bed – vein) [39]. Tumor cells secure their access to oxygen and nutrition by the formation of new blood vessels through the process of angiogenesis [40,41]. The neovascular organization depends upon various factors such as tumor type, growth rate, and location within the tumor mass. The morphological changes of the preexisting vasculature and neovasculature result in a chaotic vasculature in terms of spatial distribution such as branching, length, and diameter [42]. Bifurcation of a small microvessel into two, and even trifurcation, result in tortuous and looped structures and disorganized interconnections. Unlike normal vessels, the direction of blood flow alternates to a large extent. In addition to this chaotic vessel organization, rapidly proliferating cancer cells create solid stress onto blood vessels compressing and/or causing them to collapse [43]. The rapid growth of tumors can also result in tumor cells forcing blood vessels apart, increasing the distance between them.

Various types of tumors have been examined during and after sonopermeation to investigate the effect on vasculature and perfusion. The treatment can induce vascular damage and blood flow disruption, and eventually reduce tumor growth and prolong survival (Fig. 2). Studies describing the effect of US and MBs on the vasculature are listed in Table 1.

Wood et al. have in multiple studies investigated the effect of low-intensity FUS on tumor vasculature in mice in the presence of circulating MBs [44–48]. In a subcutaneous melanoma model, an acute reduction in tumor vascularity was observed, which persisted for 24 h [45]. Disrupted vascular walls and tumor cell death in the areas of vascular congestion and thrombosis were observed. Higher frequencies amplified heating of the tumor and led to even greater disruption of the vasculature [46]. The observed reduction in tumor vascularity was accompanied by histological findings of dilated capillaries and hemorrhage. US imaging showed that the decreased tumor vascularity (30 min and 24 h after sonication) was accompanied by an increase in echogenicity because the tumor became more disorganized, and that tissue inhomogeneities increased backscattering from the tumor [47]. Wood et al. also observed that such anti-vascular treatment could delay tumor growth and increase survival time in mice with melanoma [48].

Similar effects were observed by Goertz et al. [49–51] (Fig. 2). They studied the effects of low-intensity pulsed FUS and MBs in subcutaneous tumors in mice [50]. They observed both transient (<15 min) and sustained (2 and 24 h after repeated treatment) blood flow reduction, especially in central tumor regions, probably due to the more fragile neovascular vessels. Tumor perfusion was recovered one week after the treatment [51]. Moreover, a significant growth delay was observed in treated tumors (only FUS and MBs, no drug) relative to control tumors, suggesting that the flow modifications could have therapeutic applications

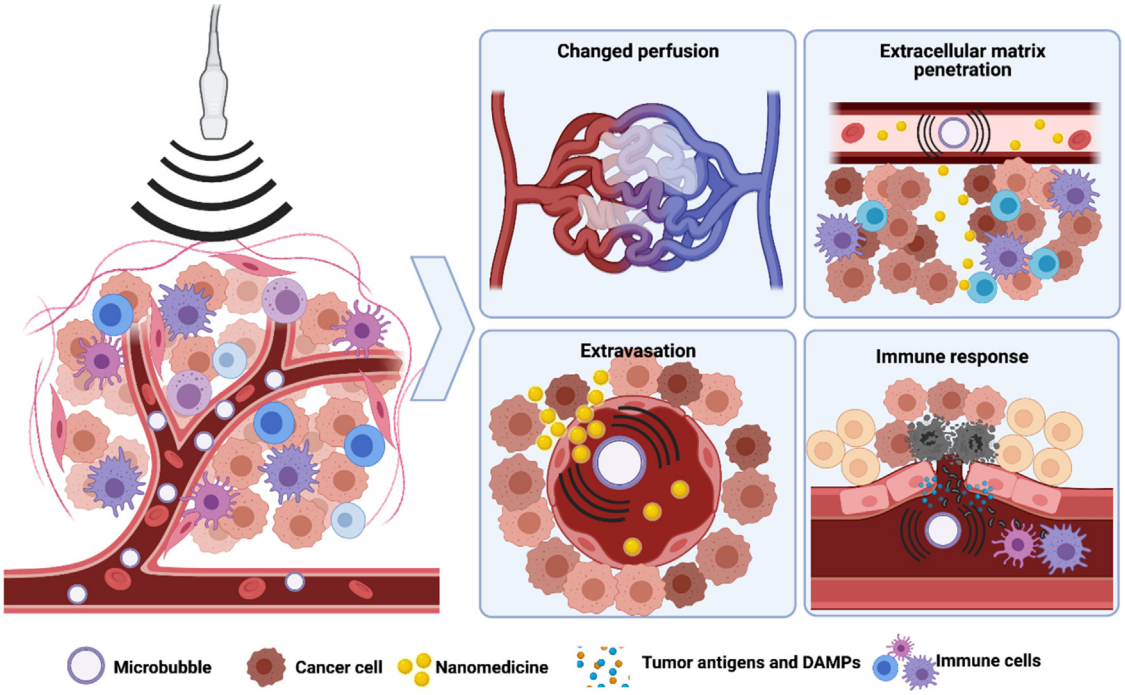

Fig. 1. Schematic illustration of possible effects of ultrasound (US) and microbubbles (MBs) in solid tumors. US focused toward the tumor causes the MBs to oscillate. This leads to changed perfusion and induction of nanomedicine extravasation followed by penetration into the extracellular matrix. The oscillating MBs can also induce an immune response by triggering release of damage-associated molecular patterns (DAMPs).

[51]. They also demonstrated that the acute reduction of tumor perfusion resulted in enhanced necrosis and apoptosis after 24 h [49].

A temporary disruption of tumor blood flow after treatment with US and MBs was also observed by Chin et al., which lasted for about 10 min when perfusion was again restored. The sonicated tumors displayed reduced growth compared to controls, while no significant temperature increase was detected [52]. An induced inflammatory response in the treated area was suggested as a possible reason for the reduced tumor growth. The treated tumors also displayed darkening and toughening of the skin and sometimes ulceration.

When treating rat glioma implanted subcutaneously in mice with US and MBs, Burke et al. observed that tumor blood flow was significantly reduced directly after treatment [53]. They hypothesized that the mechanical stress from the MBs damaged the microvasculature and observed that the reduction in tumor perfusion increased with increasing duty cycle, probably because the hydraulic resistance of the tumor microcirculation was increased due to microvessel ablation. Seven days after treatment, they observed tumor necrosis and apoptosis, and tumor growth was inhibited for the treated tumors compared to the control tumors. The authors suggested that the reduced blood flow would affect the transport of oxygen and nutrients, and thereby the number of viable tumor cells. Alternative mechanisms, according to Burke et al., could be that cavitation directly induced tumor cell damage through jet streams or shear stress, that apoptosis was initiated by oxygen free radicals, or that MB destruction triggered signals which elicited a systemic antitumor response through an immune response. Hunt et al. also hypothesized that an immune response was induced after a reduction in perfusion [54]. They observed that treatment with US and MBs in murine melanoma reduced perfusion, resulting in tumor hypoxia and ischemia-mediated cytotoxicity, increased infiltration of T-cells, and thereby intratumoral immune activation in addition to potential small-molecule retention.

Regions of reduced blood flow were observed immediately after treatment by Hu et al., who used MBs conjugated with integrins binding to endothelial cells in a breast cancer model in mice [55]. They suggested that the rapid onset limited possible mechanisms such as macrophage recruitment or changes in protein expression. They observed platelet activation and aggregation, likely resulting from the injury of small numbers of endothelial cells, and suggested these events as the mechanism for the flow reduction. They also observed that flowing MBs did not reduce blood flow at the same acoustic pressure as bubbles binding to the epithelium. Hemorrhage was not induced by the treatment, and the blood flow was observed to recover 30 min after treatment. These findings are also supported by Hwang et al., who observed that MBs could damage the endothelial surface of veins in rabbits, with most of the surface covered with adherent platelets and fibrin, an important step in the coagulation cascade. They hypothesized that this effect could be used in sclerotherapeutic thrombogenesis [56].

Kaffas et al. treated subcutaneous murine fibrosarcoma with US and MBs before radiotherapy [57]. They observed rapid vascular disruption, which lasted up to 72 h and additional therapeutic effects from sonopermeation, presumably due to reduced oxygen delivery. In contrast, Daecher et al. demonstrated that treatment with US and MBs markedly reduced tumor vascularity, but without decreasing tumor oxygenation, and used this to improve the response to radiotherapy [58]. Yemane et al. observed that treatment with US and MBs could slow down flow velocity and alter blood flow direction in tumors in dorsal window chambers [59]. Similarly, Wu et al. observed that US-mediated destruction of MBs could block circulation in tumors for 30 min, and that the blood flow was restored after 1 h [60].

FUS and MBs have also been reported to enhance blood flow by opening capillaries and increasing angiogenesis in tumors and other tissues. Vasodilation and locally increased perfusion were reported in ischemic tissues [61,62]. Bertuglia observed that US and MBs caused vasodilation and increased blood flow in hamster

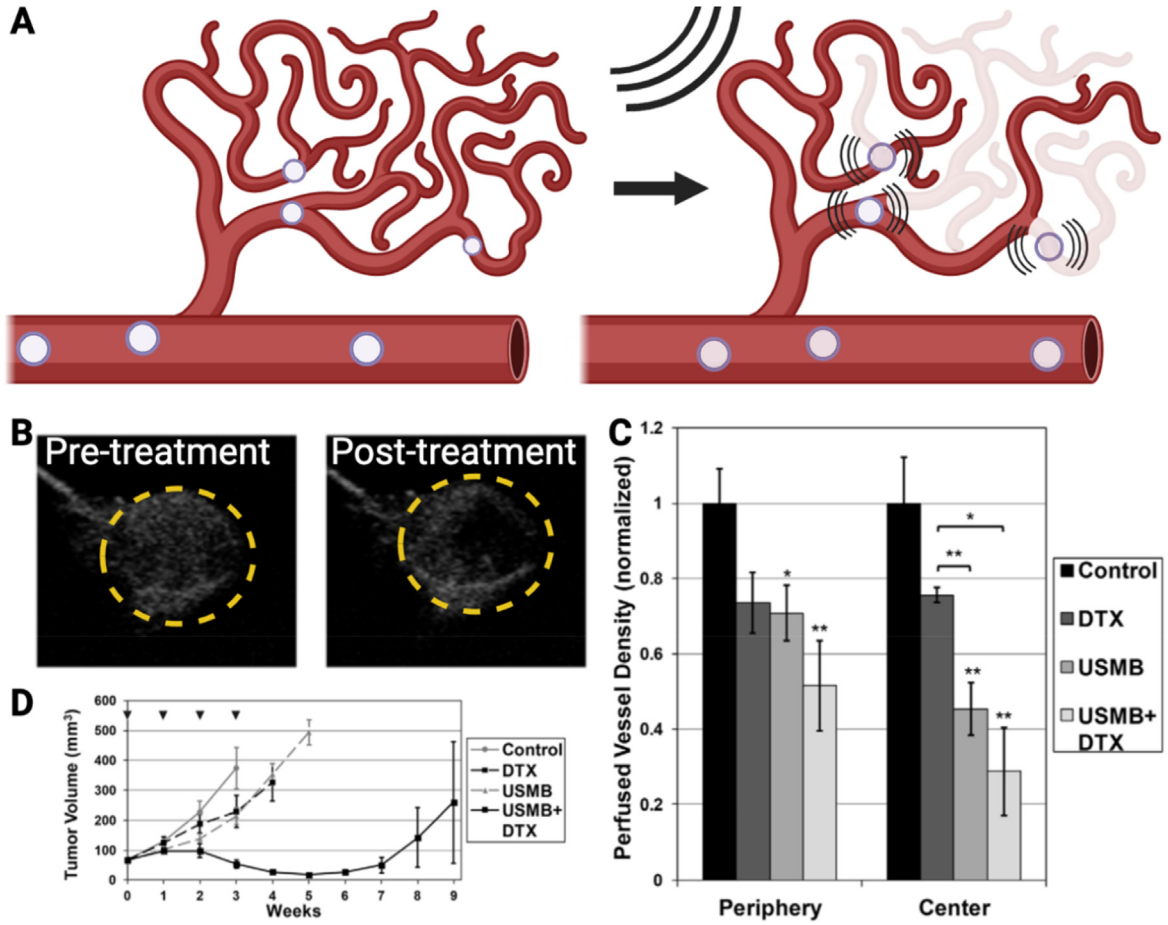

Fig. 2. Ultrasound (US) and microbubble (MB) treatment can reduce blood flow in tumors. (A) Schematic illustration of reduced perfusion due to sonopermeation. (B) US contrast images pre and post US exposure, displaying reduced contrast, especially in the central part of the tumor, and quantification of perfused vessel density (C), * indicates statistical significance. (D) The reduced perfusion resulted in delayed tumor growth. DTX = docetaxel. Figure reprinted with permission from Goertz et al. [49].

cheek pouch microcirculation. The author concluded that the effect was likely related to nitric oxide (NO) release mediated by shear stress or due to mechanical interactions leading to increased intracellular mechano-transduction in the endothelium [62]. Belcik et al. also reported that US combined with MBs could enhance perfusion in ischemic skeletal muscle both minutes and days after treatment [61]. They demonstrated that the increase was likely mediated by increased NO production and endothelial nitric oxide synthase (eNOS) phosphorylation, supporting the notion that the MBs potentiate shear-mediated endothelial response. In another study, shear dependent increase in adenosine triphosphate (ATP) from both endothelial cells and erythrocytes was found to elevate perfusion for up to 24 h [63].

Song et al. investigated the effect of US-induced MB cavitation on angiogenesis in ischemic skeletal muscle in mice seven days after treatment [64]. They observed newly generated blood vessels and concluded that the treatment caused mild damage to the endothelial cells in capillaries, resulting in transient inflammation, which could activate endothelial cells, up-regulate P-selectin and ICAM-1 expression, induce secretion of VEGF, and promote angiogenesis in the lower limb [64].

Repeated injections of targeted MBs and US imaging were found to increase the peak signal enhancement in tumors [65]. It was suggested that it could be due to increased binding of bubbles to the capillaries because of increased exposure of target sites, the mechanical opening of not yet perfused capillary tips, or extravasating bubbles after endothelial damage. The same group also observed that contrast-enhanced US imaging could enhance tumor vascularization, perfusion, and angiogenesis in breast cancer patients [66].

To summarize the possible mechanisms for reduced perfusion short time after FUS and MB exposure, most studies point towards damaged vessels and disrupted capillary walls caused by the effects from cavitating MBs on the vessel wall. The newly formed tumor vessels seem to be more fragile than vessels in normal tissue [50]. Another explanation is platelet activation and aggregation. FUS and MBs can also open vessels and induce angiogenesis, resulting in enhanced perfusion. However, the effects on perfusion depend on the US treatment, the type of tissue and vascular structure, and the type of MB used.

2.2. Increased extravasation

Another manifestation of the abnormality of tumor vessels is a defective and leaky endothelium that highly influences the internal environment of the tumor [67,68]. The endothelial cells do not form a normal endothelial layer due to their disorganization and irregular shape, and inter-endothelial gaps are frequently observed. Furthermore, the pericytes lack proper association with endothelial cells [69], and the basement membrane lacks normal connections with both endothelial cells and pericytes.

The hyperpermeable tumor capillaries and lack of functional lymphatic vessels in tumors led to the concept of the EPR-effect [3,70]. The use of nanomedicine for enhanced accumulation of

Table 1
Summary of studies describing the effect of ultrasound (US) and microbubbles (MBs) on the vasculature, extravasation into extracellular matrix (ECM) and the immune response.

Article	P_{neg}[1]	f_c[2]	t_t[3]	PRF[4]	t_p[5]	DC[6]	MB[7]	Comment
Belcik [61]	0.68, 1.48	1.3	10	9.3			LM	Increased perfusion, reversed ischemia
Belcik [63]	1.48	1.3	10	9.3			LM	Increased perfusion, reversed ischemia
Bertuglia [62]	2	2.5	15		0.0004		L/SV	Vasodilation and increased blood flow
Bulner [96]	1.65	1	2	1, 0.05	0.1*50		LM	Enhanced efficacy of immunotherapy and reduced tumor growth
Burke [53]	1–1.2	1	60	0.0002	0.1–10*5	0.01–0.00002	PM	Reduced blood flow, reduced tumor growth, increased apoptosis/necrosis
Chen [97]	0.8–7.2	1			0.002		LM	Blood vessel distention and invagination due to cavitation
Chen [98]	0.36–0.7	0.5	1.5	0.001	100		SV	Interleukin delivery, immune response, and improved treatment
Chin [52]	5	1.2	<1	0.001, 0.00005	83.3*10*3		LM	Disrupted blood flow, reversed at 10 min, inflammatory response, reduced growth
Daecher [58]	2.5	4.2	2–3	0.038	0.0016		O	Reduced tumor vascularity
Goertz [49]	1.65	1	3	1, 0.05	0.1*50	0.00024	SM	Reduced tumor perfusion, increased necrosis, and apoptosis
Goertz [50]	0.74	1	2	1, 0.05	0.1*50	0.00024	D	Transient (<15 min) and sustained (2 h and 24 h) blood flow reduction
Goertz [51]	0.74	1	3	1, 0.05	0.1*50	0.00024	D	Antivascular effects, induced tumor growth delay
Hancock [99]	8.95	1, 10	13	0.001		5		Transiently increased permeability of tissue
Hu [55]	2, 4	5	0.015	0.124	0.0012		V	Reduced perfusion, platelet activation
Hunt [54]	0.22	3	1, 3			100	D	Reduced perfusion, increased hypoxia, immune response and immune cell infiltration
Hwang [56]	1–9	1.13	1	0.005	0.38	0.22	O	Damage to endothelial surface, covered with platelets
Kaffas [57]	0.57	0.5	5	3	5	0.25	D	Vascular disruption up to 72 h
Keravnou [100]	1.7–4	1	15	0.0001	0.02, 1	2–8	LM	Reduced blood flow
Kwan [28]	1.5	0.5	12	0.0005			NC	Prolonged cavitation and increased extravasation
Lee [101]	(5–10)*	1.5	10	0.001		5		Mechanical effects induced ECM remodeling in tumors
Li [102]	1.6–17	1.1, 1.5	1	0.001	1	0.1		Enhanced drug uptake and disruption of collagen fibers
Lin [11]	1.2	1	2	0.001	10	1	SV	Increased extravasation and penetration into ECM
Liu [103]	0.6–1.4	0.5	0.33*9–12	0.001	100		SV	Suppressed tumor growth, infiltration of cytotoxic T-cells
Olsman [79]	0.4, 0.8	1	2	0.0005	10		SV	Increased extravasation and penetration into ECM
Sekino [104]		1.5	20	1				Regenerated cartilage matrix in chondrocytes
Snipstad [60]	0.1–1	1	2	0.01, 0.0005	10	2.5	NPM	Increased extravasation and penetration into ECM
Song [64]	(2)*	1	2			20	SV	Mild damage to endothelial cells, inflammation, and angiogenesis
Song [105]	(2)*	1	2			20	SV	Inflammatory signaling after MB destruction
Suen [106]	(0.002–1.8)*	0.04	0.5			100		Did not change the collagen arrangement across the sclera
Suzuki [107]	(0.7)*	1	1				BL	Interleukin delivery, T cell migration, and reduced tumor growth
Theek [80]	3.6	16	10				MM/PoM	Increased extravasation and penetration into ECM
Van Wamel [85]	0.6, 0.14	2.25, 0.5	0.75, 5	1	0.016		ACT	Increased extravasation
Wang [81]	1.7–6.9	1.8	1	0.1	0.0028		LM	Increased penetration into ECM
Watson [108]	1.1, 2.4	1.5	2, 7, 18	0.1–5	0.067			Increased nanoparticle delivery and reduced intratumoral pressure
Wischhusen [109]	5.4	1.8	5				LM	Delivered microRNA-loaded nanoparticles to tumor
Wood [45]	(2.28)*	1	1, 2, 3			100	O	25% reduction of tumor vascularity for 24 h
Wood [46]	(2.2–2.4)*	1, 3	3			100	D	Higher frequency amplified heating and vascular disruption
Wood [47]	(2.1)*	1, 2, 3	3, 6			100	D	Decreased tumor vascularity and increased echogenicity
Wood [48]	(2.4)*	3	3			100	D	Antivascular treatment delayed tumor growth and increased survival
Wu [60]		1	5	0.1		50	LM	Blocked circulation for 30 min, restored after 1 h
Xiao [110]	1	1	10	0.01		0.2	X	Reduced interstitial fluid pressure and improved drug penetration in tumors
Yan [83]	1.9	2.25	10	0.001	10	1	NPM	Increased extravasation
Yang [111]	0.5	1	1	0.001	10	10	USp	Enhanced accumulation of natural killer cells in tumors
Yemane [59]	0.2–0.8	1	5	0.0005, 0.0001	10		NPM	Slower blood flow, altered blood flow direction, and extravasation
Zhang [112]	1, 3, 5	1	5	0.01		0.2	LM	No change in collagen morphology in rabbit tumors
Zolochevska [113]	0.12	1	2	0.002		50	SV	Cytokine delivery, reduced tumor growth

[1] Peak negative pressure [MPa], * indicates intensity in W/cm^2.
[2] Center frequency [MHz].
[3] Total treatment duration [min].
[4] Pulse repetition frequency [kHz].
[5] Pulse duration [ms].
[6] Duty cycle (%).
[7] If experiments were conducted with MBs; L – Levovist, O – Optison, D – Definity, SV – SonoVue, NC – Nanocups, V – Visistar (targeted), MM – MicroMarker, LM – lipid MBs, PM – protein MBs, NPM – nanoparticle MBs, PoM – polymeric MBs, SM – surfactant MBs, ACT – Acoustic cluster therapy, BL – bubble liposomes, USp – USphere MBs.

drugs in tumors is based on the EPR-effect, enabling nanomedicines to extravasate across the capillary wall. However, the EPR-effect has shown to be heterogeneous both within tumors and between tumor types [71]. Furthermore, there are indications that the EPR effect is more pronounced in fast-growing preclinical xenograft models than in human tumors in patients [72,73], questioning whether the effect has clinical relevance. To bridge this gap between preclinical and clinical tumors, Hansen et al. studied the EPR effect in dogs with spontaneous tumors [74]. Six out of seven carcinomas retained the intravenously injected liposomes, whereas this occurred only in one out of four sarcomas, demonstrating the heterogeneity in the EPR-effect between tumor types. In clinical practice, the vascular permeability should be measured to identify patients that will benefit from cancer therapy using drug-loaded NPs [75–77].

NPs and drugs might cross the capillary wall transcellularly or paracellularly. Hydrophobic drugs can cross the plasma membrane by passive diffusion, whereas hydrophilic drugs and NPs require another mechanism, and endocytosis is reported to be an efficient cellular uptake mechanism for NPs [78]. Recently, an extensive study by Sindhwani et al. revealed that 97% of the circulating NPs crossed the capillary wall in mice in an active transport process through the endothelial cells and not through gaps between the endothelial cells [4]. This behavior was confirmed in various tumor models and using NPs of different sizes.

Increased accumulation of various types of nanomedicine in tumors exposed to FUS and MBs has been reported in many studies, and is suggested to be caused by enhanced vascular permeability. Studies describing the effect of US and MBs on extravasation of intravenously injected nanomedicine are listed in Table 1, and two examples are presented in Fig. 3. Liposomes (Doxil) (diameter approximately 80 nm) have been in clinical practice for more than 30 years. When exposed to FUS and the MB SonoVue, increased tumor uptake of liposomal doxorubicin has been demonstrated in subcutaneously growing colorectal adenocarcinoma [11] and subcutaneously growing prostate adenocarcinoma [79]. Liposomes injected immediately after administration of polymeric MBs (shell of poly(butyl cyanoacrylate)) followed by FUS, also demonstrated enhanced uptake in both pancreatic adenocarcinoma and epidermoid carcinoma with a high and low stromal content, respectively [80] (Fig. 3). In addition to liposomes, polymeric NPs are commonly used, and PLGA NPs (poly(lactic-co-glycolic acid), diameter 116 nm) were found to increase their penetration into the ECM of colon tumors after US treatment [81]. Furthermore, NPs on the surface of MBs, either directly forming the shell [32] or conjugated via a biotin-avidin linker [82], show potential for enhanced delivery of NPs. Polymeric NPs on the shell of MBs in a solution with excess of free polymeric NPs (poly(alkyl cyanoacrylate), diameter 150 nm) showed increased uptake in subcutaneously growing tumors after exposure to FUS [8,12]. Liposome-MB complexes

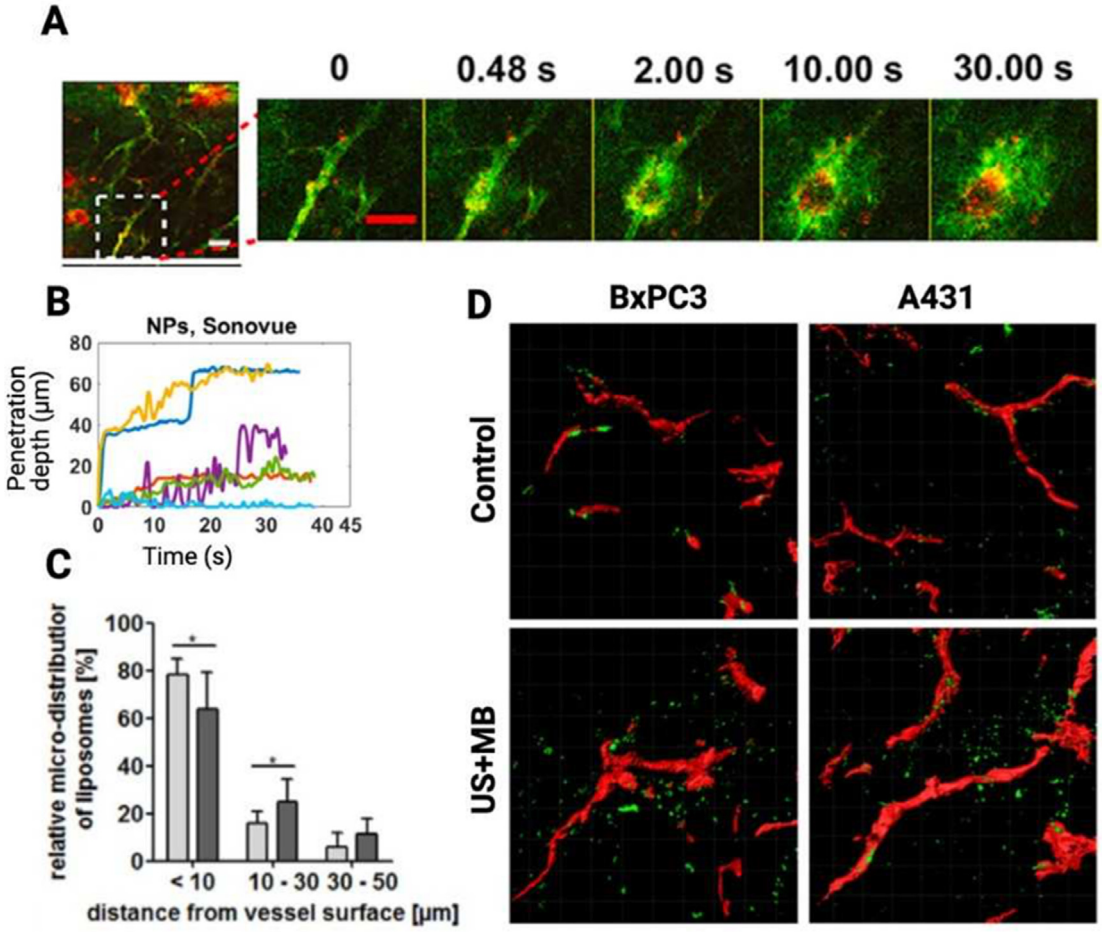

Fig. 3. Sonopermeation with ultrasound (US) and microbubbles (MBs) causes increased extravasation and penetration of nanoparticles (NPs) into extracellular matrix (ECM). (A) In vivo multiphoton imaging of NPs (red) and 2 MDa dextran (green) as a function of time after onset of US. The images show the kinetics of extravasation and penetration into the ECM. (B) Extravasation distance quantified as a function of time. Figures A and B reprinted with permission from Yemane et al. [59]. (C) Distribution of NPs as a function of distance into the ECM, treated tumors (dark grey) showed more NPs penetrating further into ECM than controls (light grey). * indicates statistical significance. (D) Confocal laser scanning microscopy of tumor tissue showing blood vessels (red) and NPs (green). Figures C and D reprinted with permission from Theek et al. [80].

loaded with paclitaxel also showed four-fold increased uptake of paclitaxel into tumor tissue after exposure to FUS compared to free paclitaxel and FUS [83]. Another promising approach for enhanced drug delivery is novel MB platforms with prolonged circulation time and cavitation activity. Acoustic Cluster Therapy (ACT®) generates large MBs through a phase shift of microclusters. The MBs have a typical diameter of 25 μm and stay in the circulation for up to 10 min [84], and combined with FUS were found to increase uptake of the PEGylated macromolecule 800CW-PEG (25–60 kDa) in a subcutaneous prostate cancer model [85]. Cup-formed NPs (diameter 180–600 nm) entrapping surface nanobubbles demonstrated cavitation activity for several minutes; Kwan et al. showed that nanocups and FUS increased the delivery of fluorescent antibodies into ECM in tumors, and the nanocups did also extravasate [28]. Although FUS and MBs improve extravasation of NPs, there are examples where macromolecules might not need FUS and MBs for successful extravasation. Intravenously injected Evans blue, which binds to albumin, extravasated efficiently due to the EPR effect, and applying US and MBs did not significantly improve the accumulation in subcutaneously growing colon adenocarcinoma [86]. However, in hepatoma using a similar US exposure regimen, FUS and MBs enhanced the accumulation of Evans blue-albumin in tumor tissue four-fold compared to Evans blue-albumin alone [87], demonstrating the heterogeneity in vascular permeability.

More direct evidence of how MBs and NPs behave during US exposure can be obtained by intravital microscopy. In tumors growing in dorsal window chambers, real-time intravital microscopy during FUS exposure was performed [59] (Fig. 3). It was demonstrated that extravasation occurred mainly in vascular branching points, probably due to retention of MBs at such locations or because the vessel wall is more fragile near the branching points. Smaller vessels were found to require higher acoustic pressures to achieve extravasation than blood vessels with larger diameters. Extravasation occurred throughout the 5 min US exposure and were observed milliseconds to minutes after the onset of US exposure. It was suggested that differences in blood vessel density, organization, branching, and blood flow velocity can cause fluctuations in the amount of MBs in the region exposed to FUS, thereby affecting the location and onset time of the extravasation [88].

While improved extravasation after sonopermeation is well documented, the exact mechanisms are not clear, but biomechanical effects on the vessel wall generated by the oscillating MBs are likely important. Caskey et al. reported that the oscillating MBs formed tunnels in agarose gels with stiffness similar to soft tissue [89], indicating a mechanism for increasing permeability of the capillary wall. The tunnels were formed in the direction of the propagating US wave and had a width up to 35 μm, depending on the frequency and acoustic pressure. Oscillating MBs are shown to cause microstreaming and shear stress. High-speed imaging of the oscillating MBs suggests a "push–pull" mechanism of the endothelial wall [90]. In addition, when the MB collapses in the violent process of inertial cavitation, jet streams are formed that can generate pores in the endothelial cells or increase the opening between the endothelial cells [19,21,23].

Neither intravital microscopy nor the other in vivo studies mentioned above distinguished between paracellular and transcellular extravasation. US and MBs are reported to enhance endocytosis [91,92], thus transcellular passage through the endothelial cells can take place both as a result of enhanced endocytosis and pore formation on the endothelial surface. To study the effect of oscillating MBs on the endothelial layer and distinguish between transcellular and paracellular extravasation, most studies have been done in vitro using monolayers of cells, microfluidics, or gel phantoms [93–95].

To summarize the mechanisms of US-enhanced extravasation, MBs oscillating close to the endothelial layer can cause microstreaming, shear stress, jet streams, or shock waves, which increase the space between the endothelial cells, form pores in the plasma membrane of the endothelial cells, and increase endocytosis.

2.3. Modifying the extracellular matrix and altering tumor pressures

After extravasation from the blood vessels, nanomedicines and drugs must penetrate through the ECM to reach the cancer cells. ECM can be a major component of solid tumors and can comprise up to 60% of the tumor mass [114]. In tumors, the organization and composition of the ECM differ from normal tissue [114]. The three main constituents of ECM are collagen fibers, proteoglycans, and glycosaminoglycans (GAGs) such as hyaluronan [115,116]. Type I and III collagen are the most abundant ECM components and provide tensile strength to the tumor [115,117–120], while hyaluronan resists compression [121]. Thus, the amount of collagen and hyaluronan is particularly important for tumor stiffness [122].

The network of collagen, proteoglycans, and hyaluronan results in a physical barrier limiting the transport of drugs and nanomedicines. Collagen is reported to contribute to transport resistance, and an inverse relationship between collagen content in tumors and the interstitial diffusion of large macromolecules has been found [123]. Hyaluronan is important for hydraulic conductivity, which determines the interstitial flow through the network of pores in the ECM, and hydraulic conductivity is less influenced by the amount of collagen [124].

Cancer-associated fibroblasts (CAFs) are the main cells responsible for changing the ECM composition of the tumor stroma [125,126] and are associated with resistance to therapeutic drugs [127,128]. Through interaction with tumor cells, CAFs can upregulate production of ECM components and induce structure modifications and remodeling [129]. Hence, many ECM constituents are overexpressed and cross-linked, which results in a denser and stiffer ECM in tumors compared to normal tissue [114,117].

The rapid, uncontrolled proliferation of cells constrained by a dense ECM can further hamper delivery of nanomedicine and drugs in the tumor interstitium by increasing the tumor pressure. Elevated pressure is present in most tumors [130–132] and can be categorized into solid stress and interstitial fluid pressure (IFP) [133]. Solid stress arises from non-fluid elements in the tumor bulk. As the densities of cancer cells, stromal cells, and ECM constituents increase within the restricted environment of the host tissue, solid stress might develop [134]. It has been shown that solid stress is related to tissue stiffness [122], but it should be noted that these quantities are distinct mechanical properties of the tumor [135]. The solid stress compresses compliant structures, such as blood vessels and lymphatic vessels in the tumor interior. Compressing blood vessels blocks oxygen, nutrient and drug supply to the tumor [43,136]. On the other hand, compressing lymphatic vessels reduces tumor drainage and increases IFP [121,137]. Therefore, the accumulation of solid stress limits both vascular and interstitial transport.

The fluid and plasma leaking from hyperpermeable blood vessels into the interstitial tumor space are unable to drain or percolate to the surrounding normal tissue due to the dysfunctional lymphatic system and dense ECM [138]. Thus, excess fluid accumulates in the tumor interstitium, and the IFP increases to the level of microvascular pressure [139,140]. The increased IFP eliminates fluid pressure gradients and consequently limits movement of drugs through convection, rendering diffusion the main mechanism of delivery of drugs and nanomedicine in tumor interstitium [115–117,138]. Alleviation of solid stress and IFP by a range of

chemical and physical treatments has been demonstrated to improve drug delivery to the tumor interstitium [141–145].

FUS and circulating MBs are shown to improve the penetration of NPs and drugs into the interstitium [8,9,11,79,80] (Fig. 3). The average penetration of NPs from the blood vessel wall is in several studies found to be in the range of 50–60 μm, whereas the penetration without FUS is typically 10–30 μm [59,79,80] (Fig. 3). Combining US and MBs allows for local cavitation of the MBs in the vessels, leading to mechanical effects on the capillary wall. However, it is not clear how MBs, being constrained in the vasculature due to their size (diameter 2–3 μm), can affect the tumor ECM. Using high-speed imaging, Chen et al. observed that MBs, oscillating in the capillaries, correlated with vessel distention and invagination, indicating vessel oscillation [97]. This can potentially affect the perivascular area, improving delivery of drugs through the ECM, as observed by the perivascular pump driven by arterial pulsation [146]. This is clearly a topic that needs further investigation.

The successful delivery of NPs clearly demonstrates that sonopermeation facilitates transport through the ECM, suggesting remodeling of the ECM. Studies describing the effect of US and MBs on ECM are listed in Table 1. To our knowledge, there is only one study reporting a correlation between enhanced drug uptake and disruption of collagen fibers [102]. Li et al. demonstrated that when applying pulsed high-intensity FUS and MBs in a pancreatic transgenic mouse model, enhanced tumor uptake of doxorubicin was observed in tumor areas displaying damaged collagen fibers [102]. The collagen fibers seemed disorientated and fringe, and the dense collagen bundles were separated.

As most MBs will not enter the ECM, studies applying FUS without MBs can also be helpful for providing information on whether FUS influences ECM composition and structure. Studies in both tumor and non-tumor tissue have been reported. Pulsed high-intensity US decreased the amount of collagen in lung carcinoma in mice, which correlated with increased tissue penetration of NPs [101]. Furthermore, in calf muscle in mice, high-intensity FUS increased the penetration of NPs, and gaps between the muscle fiber bundles were observed. The gaps were transient, they appeared largest immediately after US exposure and disappeared after approximately three days. These observations were explained by the weak connections between muscle fiber bundles being exposed to shear strain induced by acoustic radiation force. Thermal effects could not explain the gaps [99]. Low-intensity pulsed US has shown promising effects in articular cartilage, particularly for chondrocytes in patients with osteoarthritis, and might be used in bone healing. One possible mechanism is that US induces cartilage matrix synthesis and an increase in collagen II. Remodeling of the proteoglycan aggrecan and a decrease in the expression of metalloproteinases have been found [104]. Low-intensity pulsed US is also reported to deliver macromolecules to the posterior segment of the eye via the transscleral route. Sclera consisting of collagen fibrils, proteoglycans, and elastin, represents a delivery barrier, and US was shown to increase the scleral permeability for macromolecules, whereas the scleral collagen fiber arrangement remained unchanged [106]. The collagen fibers were measured three days after treatment by the second-harmonic generating (SHG) signal, and potential changes in the collagen structure might not be detectable at this optical spatial resolution and late time point.

Enzymatic degradation of collagen [101] and hyaluronan [147] reduces IFP in tumors growing in mice and improves tumor uptake of macromolecules and liposomes. However, it is unclear whether US exposure relevant for US-mediated delivery of drugs will change IFP. There are two studies using high US intensities reporting changes in IFP. Zhang et al. reported that US and MBs changed the IFP depending on the US pressures [112]. For the lowest (1 MPa) acoustic pressure, the IFP increased somewhat, while the middle (3 MPa) and highest pressure (5 MPa) decreased IFP. The reduction in IFP was reported to occur without any significant changes in the collagen structure and content. However, heterogeneity in collagen structure and limited spatial resolution might hamper the detection of any changes in the collagen structure. Interestingly, increasing amount of collagen fibers was found to correlate with increased IFP. In a similar study using the same US parameters except increasing exposure time from 5 to 10 min, Xiao et al. reported that 1 MPa US in combination with MBs reduced IFP and improved drug penetration [110]. MBs were needed to observe any reduction in IFP, as US alone did not change the IFP [112]. As US exposure for more than 5 min will probably destroy all MBs, the reduction in IFP observed by Xiao et al. could be caused by hyperthermia. US-induced hyperthermia increasing the temperature up to 42 °C for 5 min was found to reduce the IFP [108]. In this study, US also reduced IFP after the mice were euthanized, and the authors suggested that the reduction in IFP was not solely caused by changes in blood flow but likely due to changes in the ECM. Measuring potential changes in IFP using US exposures clinically relevant for drug delivery is needed.

No papers have been published to uncover the effect of US and MBs on solid stress. Nieskoski et al. showed that solid stress constituted the major part of the overall tumor pressure compared to IFP [148]. The relationship between stroma, IFP, and solid stress indicates that sonopermeation could alter solid stress.

To summarize the mechanisms of US-improved penetration of nanomedicine throughout the ECM, oscillating MBs can cause the capillary wall to oscillate and improve transport in the perivascular space, and the ECM and collagen structure are probably remodeled. However, more research is needed to clarify these possible mechanisms, as well as the effect of US and MBs on solid stress and IFP.

3. Inducing an immune response

It has been widely recognized that the immune system represents both a barrier to efficient cancer therapy and a therapeutic opportunity. Evading destruction by immune effector cells and maintaining a tumor-promoting inflammation are both hallmarks of cancer [149]. Tumors can be heavily infiltrated by immune cells, especially tumor-associated macrophages (TAMs) and regulatory T-cells, which downregulate cytotoxic T lymphocytes and promote both tumor growth and metastasis [150]. TAMs are also scavengers of nanomedicine and have been shown to engulf a substantial part of the nanomedicine accumulating in a solid tumor [151,152]. The presence of immune cells in the tumor is a sign of an initial immune response to cancer cells and a latent potential for immune-mediated cytotoxicity.

US has been described with multiple applications within the umbrella of immunotherapy, and its role to overcome the barrier the immune system represents was recently reviewed by Deprez et al. [38]. In the present review, we rather describe the therapeutic potential of using US and MBs to induce an immune response and efficiently deliver immunotherapeutics (Fig. 4). Studies describing immune effects induced by US and MBs are listed in Table 1. Applications of US in immunotherapy include both delivery (e.g. in vitro gene delivery, in vivo immunotherapeutics delivery) and direct effects (e.g. mechanical agitation, thermal ablation, and boiling histotripsy) as reviewed previously [38,153,154]. Sonopermeation is far less explored for immunotherapeutic applications than thermal ablation, and the current literature is not clear on the immunogenicity induced by US exposures used in drug delivery. Multiple studies have shown that violently collapsing MBs can create damage and inflammatory signaling (Fig. 4A). Liu et al. showed that sonopermeation could suppress tumor growth by causing an infiltration of cytotoxic T-cells (Fig. 4C), although using higher pres-

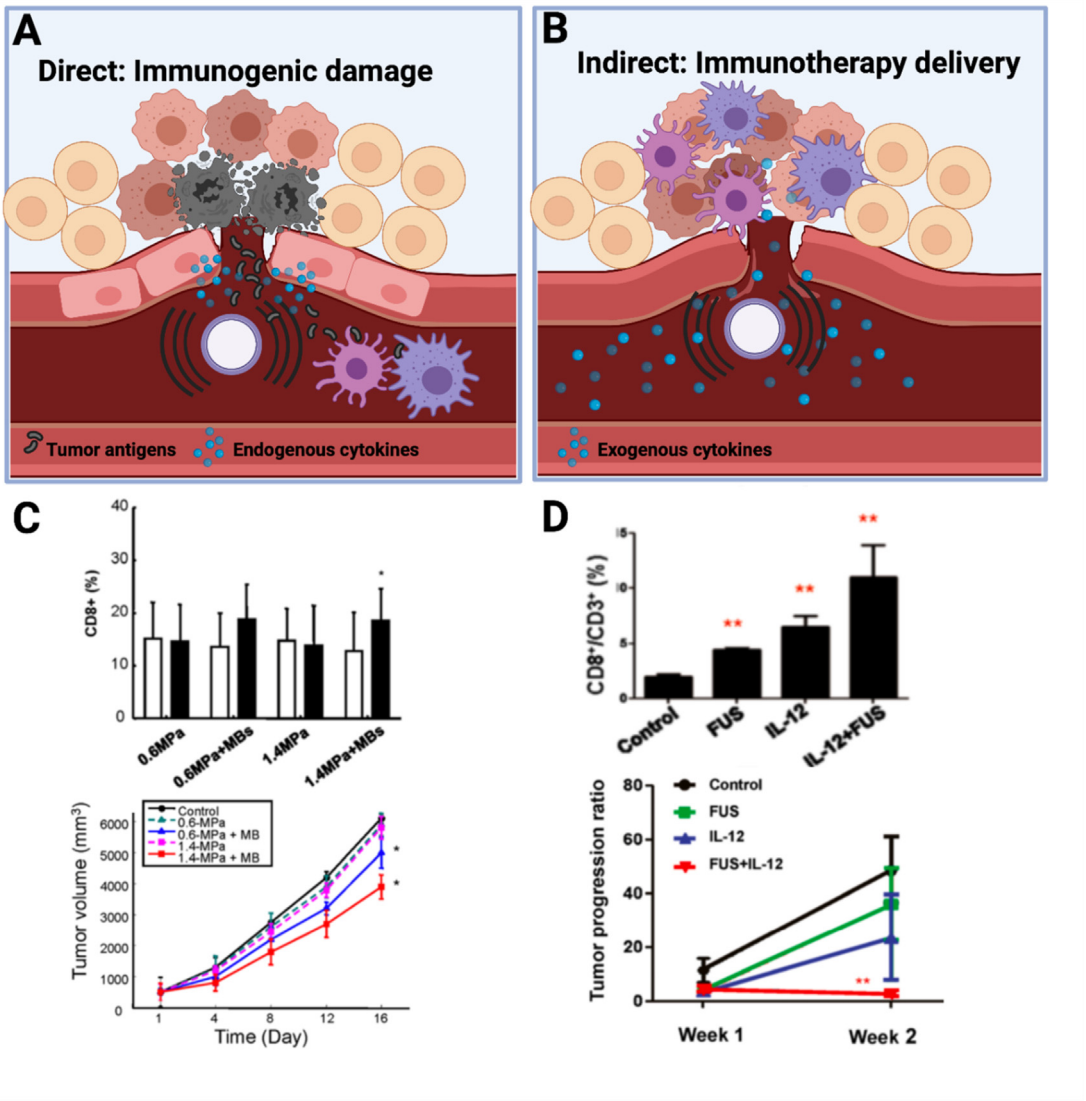

Fig. 4. Application of focused ultrasound (FUS) and microbubbles (MBs) for immunotherapy. (A) Schematic showing tissue damage from MBs creating tumor antigens and inflammatory cytokines. (B) Schematic showing delivery of exogenously administered inflammatory cytokines. (C) Increased $CD8^+$ T-cells following FUS and MBs, significantly delayed tumor growth in a murine model of colorectal cancer. Figure C adapted with permission from Liu et al. [103]. (D) Increased T-cell infiltration and impaired tumor growth after sonopermeation and administration of IL-12 in a glioma model in rats. * indicates statistical difference. Figure D adapted with permission from Chen et al. [98].

sures than used by most groups (mechanical index up to 1.4) [103]. Concordantly, Hunt et al. found that blood vessel destruction by violently oscillating MBs induced an immune response and increased T-cell infiltration in the tumor [54], Song et al. found inflammatory signaling after MB destruction in a model of ischemia [105], and Kovacs et al. showed that sterile inflammation was present in the brain after blood–brain barrier (BBB) opening with FUS and MBs [155].

The potential of US and MBs to induce immunogenicity and tumor homing by immune cells was studied by Yang et al., who showed increased tumor accumulation and therapeutic effect of adoptively transferred natural killer cells following US and MBs in a model of ovarian cancer [111]. Improved delivery or homing of adoptively transferred immune cells have also been reported in brain tumor models after BBB opening [156,157]. These few studies indicate that MBs oscillating in an US field can cause sufficient damage to induce a local immune response and should be evaluated in more detail to understand how this damage can be exploited.

An indirect way of overcoming the anti-inflammatory tumor microenvironment with US is by improving delivery of immunotherapeutics (Fig. 4B). This was recently done by Bulner et al., who combined an anti PD-1 antibody with US and MBs and achieved prolonged survival in mice with a model of colorectal cancer [96]. However, the effect was not believed to be due to improved delivery, but rather due to the effects of checkpoint inhibition in combination with destruction of the tumor vasculature by US and MBs. Other more experimental therapeutics have also been delivered using sonopermeation. Multiple groups have delivered inflammatory cytokines or cytokine-encoding genes locally and have observed increased $CD8^+$ T-cell infiltration and therapeutic benefit [98,107,109,113,158] (Fig. 4D).

It is known that induction of local damage and an immune response in a tumor can give systemic immunity and clearance of metastases by the abscopal effect from radiation therapy [159]. Studies mentioned above point in the direction that sonopermeation can create local inflammation that can trigger the release, uptake, and presentation of tumor antigens and facilitate a systemic response. This application would expand the potential

use of therapeutic US substantially and should be thoroughly investigated.

4. Clinical impact and outlook

Promising preclinical studies have initiated several clinical trials to assess the therapeutic effect of applying FUS in the presence of MBs combined with various drugs. In most of the clinical studies, the MBs injected are clinically approved contrast agents such as SonoVue or Sonazoid. Two similar ongoing studies in patients with colorectal cancer and liver metastases treat patients with standard chemotherapy, inject SonoVue and apply US towards the selected liver metastasis. The sizes of treated and untreated liver metastases are monitored by CT (ClinicalTrials.gov identifier NCT03458975 and NCT03477019). Such studies will give important knowledge to what extent US and injected MBs improve chemotherapy. Furthermore, patients with inoperable pancreatic tumors are treated with standard chemotherapy (Gemcitabine or FOLFIRINOX) in two ongoing and one to-start study (NCT04821284, NCT03458975, NCT04146441). Pancreatic tumors are characterized by a dense desmoplastic stroma forming a physical barrier that effectively hinders systemically administered drugs from reaching cancer cells. Thus, applying FUS and MBs might be a good approach to break this barrier and improve chemotherapy. In a phase 3 trial, breast cancer patients are given US and SonoVue neoadjuvant chemotherapy (NCT03385200). Additionally, enhancing the effect of ionizing radiation by FUS and intravenously injected MBs is assessed in patients with head and neck tumors (NCT04431648) and chest-wall and locally advanced breast cancer (NCT04431674). The motivation for these trials is preclinical studies demonstrating a synergistic-additive effect of radiotherapy and sonopermeation, but the mechanisms behind the sensitization are still unclear [160]. US and MBs are also used to improve radioembolization based on yttrium-80 microspheres in patients with hepatocellular carcinoma (NCT03199274). Various preclinical studies have demonstrated that FUS and MBs increase the permeability of the BBB [157,161–165], and several clinical studies to treat brain cancer are also ongoing (NCT04804709; NCT04528680, NCT04417088, NCT04440358).

Currently, only a few clinical trials have published their results. A phase I study including ten patients with inoperable pancreatic cancer treated with gemcitabine combined with SonoVue and US is completed [15]. No additional toxic effects were observed compared to gemcitabine treatment alone, and in five patients, the maximum tumor diameter decreased. Promising results were also shown in eleven patients with tumors in the digestive system and liver metastasis. The patients received chemotherapy before SonoVue was injected, and the tumor received US [16]. In addition, three phase 1–2 clinical studies opening the BBB in patients with glioma show that the BBB opening was safe and the patients tolerated the treatment [166–168].

To obtain efficient and safe translation to the clinic, there are some safety issues to consider when performing treatments with US and MBs. To have MBs circulating throughout the treatment period, multiple injections are often given. One strategy to achieve prolonged circulation could be to coat the diagnostic MBs, however, this should be avoided since coating of MBs (e.g. poly(ethylene glycol) (PEG) or avidin) is reported to induce an immune response [19,169]. Rather, novel MB platforms with long circulation times designed for therapeutic purposes should be developed. Monodisperse MBs have been shown to be very efficient as they will have a more reproducible and efficient cavitation response [38,170]. It might also be an advantage to have larger bubbles than the typical contrast agents of 2–5 μm in diameter. A larger MB will cover more of the vascular wall, and effects such as microstreaming, jet formation, and endocytosis might be enhanced [84]. Large MBs are formed through Acoustic Cluster Therapy (ACT®) based on phase-shifting of microclusters, and these bubbles can lodge in capillaries for up to 10 min [27,85]. Microsized MBs are constrained to the vasculature, whereas nanosized bubbles or bubble precursors being acoustically vaporized to undergo a phase shift into a gas bubble after entering the ECM, are an interesting approach for more efficient delivery of drugs and NPs [29–31]. Nanocups entrapping nanobubbles were shown to both extend the circulation time/cavitation activity and to extravasate into the ECM and cavitate in the proximity to the cancer cells [28]. Another approach to increase drug delivery locally could be to use actively targeted MBs, which are retained at the target [35]. Recently, several groups have also loaded the MBs with drug for increased efficacy [33,34].

Novel MBs will require different US frequencies, pulse lengths, and acoustic intensities than can be obtained using diagnostics US scanners and transducers. The optimal frequency is lower than that used in US imaging and is typically in the range of kHz to a few MHz. Larger MBs require lower frequencies closer to their resonance frequency [171]. Another advantage of using lower frequencies is that the US waves will penetrate deeper into the tissue, as less acoustic energy is attenuated [172]. Focusing the US beam also deposits the energy further into the body and within the tumor [173]. Thus, depending on the location of the tumor and the MB platform, the design of the US transducer should be optimized. Furthermore, dual-frequency transducers using a high frequency for imaging and localizing the tumor to be treated, and a lower frequency for improving drug delivery, will be useful. The optimal acoustic intensity, pulse length, and pulse repetition frequency depend on the location of the tumor and the type of MB used. These parameters need to be optimized to achieve efficient delivery of the drug while avoiding damage such as severe vascular rupture and bleeding. Including cavitation detection through real-time feedback monitoring can allow the treatment to be adjusted for each individual tumor, ensuring sufficient acoustic intensities and avoiding damage. There is clearly an urgent need for US transducers dedicated for drug delivery.

5. Conclusion

Preclinical studies demonstrate that applying US and MBs improves delivery of various therapeutic agents to solid tumors, and successful therapeutic outcomes are achieved. Two recently published clinical trials also indicate no severe side effects, and reduced tumor size in some of the patients. To optimize the treatment of cancer, it is essential to understand the underlying mechanisms and how to overcome physical barriers for successful delivery of therapeutic agents. Thus, more knowledge on the effect of sonopermeation in all steps in the delivery process is needed. This especially applies to how US and MBs facilitate transport through ECM, as this is the least studied step in the delivery process. The indications that sonopermeation induces an immune response, and possible advantages of combining sonopermeation and immunotherapy, also need further investigations. The preclinical and clinical studies have revealed large variations in the therapeutic response, and we need to know which parameters are critical for successful delivery of drugs and nanomedicine. This includes both tumor characteristics such as vascularization, blood vessel permeability, ECM composition and structure, hydraulic conductivity, solid stress, IFP, and immune status, as well as properties of the therapeutic agents. Stratification of cancer patients based on the tumor properties is essential to ensure that FUS and MBs are offered to patients that can benefit from such therapy. Fur-

thermore, optimization of US parameters and transducers must be done, and knowledge about maximum US pressures and pulses that can be applied safely are needed. MBs tailored for therapeutic purposes could improve the efficacy of the treatment. The many ongoing and planned clinical trials indicate that within the next few years, valuable new information on the efficacy of US-mediated delivery of therapeutic agents, therapeutic response, and potential side effects will be obtained, which can result in a new clinical practice for improved cancer therapy.

Declaration of Competing Interest

The authors declare that they have no known competing financial interests or personal relationships that could have appeared to influence the work reported in this paper.

Acknowledgement

The Central Norway Regional Health Authority (project 90270600) and the Norwegian Research Council (project number 26228) are acknowledged for financial support. Schematic illustrations were created with BioRender.

References

[1] H.P. Gerber, P.D. Senter, I.S. Grewal, Antibody drug-conjugates targeting the tumor vasculature Current and future developments, Mabs 1 (2009) 247–253.
[2] K.A. Kurdziel, J.D. Kalen, J.I. Hirsch, J.D. Wilson, H.D. Bear, J. Logan, J. McCumisky, K. Moorman-Sykes, S. Adler, P.L. Choyke, Human dosimetry and preliminary tumor distribution of F-18-fluoropaclitaxel in healthy volunteers and newly diagnosed breast cancer patients using PET/CT, J. Nucl. Med. 52 (2011) 1339–1345.
[3] H. Maeda, J. Wu, T. Sawa, Y. Matsumura, K. Hori, Tumor vascular permeability and the EPR effect in macromolecular therapeutics: a review, J. Control. Release 65 (2000) 271–284.
[4] S. Sindhwani, A.M. Syed, J. Ngai, B.R. Kingston, L. Maiorino, J. Rothschild, P. MacMillan, Y. Zhang, N.U. Rajesh, T. Hoang, J.L.Y. Wu, S. Wilhelm, A. Zilman, S. Gadde, A. Sulaiman, B. Ouyang, Z. Lin, L. Wang, M. Egeblad, W.C.W. Chan, The entry of nanoparticles into solid tumours, Nat. Mater. 19 (2020) 566–575.
[5] A. Shafei, W. El-Bakly, A. Sobhy, O. Wagdy, A. Reda, O. Aboelenin, A. Marzouk, K. El Habak, R. Mostafa, M.A. Ali, M. Ellithy, A review on the efficacy and toxicity of different doxorubicin nanoparticles for targeted therapy in metastatic breast cancer, Biomed. Pharmacother. 95 (2017) 1209–1218.
[6] A.C. Anselmo, S. Mitragotri, Nanoparticles in the clinic: an update, Bioeng. Transl. Med. 4 (2019) e10143.
[7] R. van der Meel, E. Sulheim, Y. Shi, F. Kiessling, W.J.M. Mulder, T. Lammers, Smart cancer nanomedicine, Nat. Nanotechnol. 14 (2019) 1007–1017.
[8] S. Snipstad, S. Berg, Y. Morch, A. Bjorkoy, E. Sulheim, R. Hansen, I. Grimstad, A. van Wamel, A.F. Maaland, S.H. Torp, C.L. Davies, Ultrasound improves the delivery and therapeutic effect of nanoparticle-stabilized microbubbles in breast cancer xenografts, Ultrasound Med. Biol. 43 (2017) 2651–2669.
[9] S. Kotopoulis, A. Delalande, M. Popa, V. Mamaeva, G. Dimcevski, O.H. Gilja, M. Postema, B.T. Gjertsen, E. McCormack, Sonoporation-enhanced chemotherapy significantly reduces primary tumour burden in an orthotopic pancreatic cancer xenograft, Mol. Imaging Biol. 16 (2014) 53–62.
[10] S. Eggen, M. Afadzi, E.A. Nilssen, S.B. Haugstad, B. Angelsen, L. Davies Cde, Ultrasound improves the uptake and distribution of liposomal Doxorubicin in prostate cancer xenografts, Ultrasound Med. Biol. 39 (2013) 1255–1266.
[11] C.Y. Lin, J.R. Li, H.C. Tseng, M.F. Wu, W.L. Lin, Enhancement of focused ultrasound with microbubbles on the treatments of anticancer nanodrug in mouse tumors, Nanomedicine 8 (2012) 900–907.
[12] S. Snipstad, Y. Morch, E. Sulheim, A. Aslund, A. Pedersen, C.L. Davies, R. Hansen, S. Berg, Sonopermeation enhances uptake and therapeutic effect of free and encapsulated cabazitaxel, Ultrasound Med. Biol. 47 (2021) 1319–1333.
[13] D. Bressand, A. Novell, A. Girault, W. Raoul, G. Fromont-Hankard, J.M. Escoffre, T. Lecomte, A. Bouakaz, Enhancing nab-paclitaxel delivery using microbubble-assisted ultrasound in a pancreatic cancer model, Mol. Pharm. 16 (2019) 3814–3822.
[14] C.W. Schultz, G. Ruiz de Garibay, A. Langer, J.B. Liu, T. Dhir, C. Leitch, C.E. Wessner, M. Mayoral, B. Zhang, M. Popa, C. Huang, S. Kotopoulis, X. Luo, Y. Zhen, S. Niu, M. Torkzaban, K. Wallace, J.R. Eisenbrey, J.R. Brody, E. McCormack, F. Forsberg, Selecting the optimal parameters for sonoporation of pancreatic cancer in a pre-clinical model, Cancer Biol. Ther. 22 (2021) 204–215.
[15] G. Dimcevski, S. Kotopoulis, T. Bjånes, D. Hoem, J. Schjøtt, B.T. Gjertsen, M. Biermann, A. Molven, H. Sorbye, E. McCormack, M. Postema, O.H. Gilja, A human clinical trial using ultrasound and microbubbles to enhance gemcitabine treatment of inoperable pancreatic cancer, J. Control. Release (2016).
[16] Y. Wang, Y. Li, K. Yan, L. Shen, W. Yang, J. Gong, K. Ding, Clinical study of ultrasound and microbubbles for enhancing chemotherapeutic sensitivity of malignant tumors in digestive system, Chin. J. Cancer Res. 30 (2018) 553–563.
[17] S. Snipstad, E. Sulheim, C. de Lange Davies, C. Moonen, G. Storm, F. Kiessling, R. Schmid, T. Lammers, Sonopermeation to improve drug delivery to tumors: from fundamental understanding to clinical translation, Expert Opin. Drug Deliv. 15 (2018) 1249–1261.
[18] P. Dayton, A. Klibanov, G. Brandenburger, K. Ferrara, Acoustic radiation force in vivo: a mechanism to assist targeting of microbubbles, Ultrasound Med. Biol. 25 (1999) 1195–1201.
[19] S. Hernot, A.L. Klibanov, Microbubbles in ultrasound-triggered drug and gene delivery, Adv. Drug Deliv. Rev. 60 (2008) 1153–1166.
[20] W.G. Pitt, G.A. Husseini, B.J. Staples, Ultrasonic drug delivery–a general review, Expert Opin. Drug. Deliv. 1 (2004) 37–56.
[21] V. Frenkel, Ultrasound mediated delivery of drugs and genes to solid tumors, Adv. Drug Deliv. Rev. 60 (2008) 1193–1208.
[22] M. Afadzi, O.F. Myhre, P.T. Yemane, A. Bjorkoy, S.H. Torp, A. van Wamel, S. Lelu, B.A.J. Angelsen, C. de Lange Davies, Effect of acoustic radiation force on the distribution of nanoparticles in solid tumors, IEEE Trans. Ultrason. Ferroelectr. Freq. Control 68 (2021) 432–445.
[23] G.A. Husseini, W.G. Pitt, A.M. Martins, Ultrasonically triggered drug delivery: breaking the barrier, Colloids Surf. B Biointerfaces 123 (2014) 364–386.
[24] K. Kooiman, S. Roovers, S.A.G. Langeveld, R.T. Kleven, H. Dewitte, M.A. O'Reilly, J.M. Escoffre, A. Bouakaz, M.D. Verweij, K. Hynynen, I. Lentacker, E. Stride, C.K. Holland, Ultrasound-responsive cavitation nuclei for therapy and drug delivery, Ultrasound Med. Biol. 46 (2020) 1296–1325.
[25] M. Versluis, E. Stride, G. Lajoinie, B. Dollet, T. Segers, Ultrasound contrast agent modeling: a review, Ultrasound Med. Biol. 46 (2020) 2117–2144.
[26] E. Stride, T. Segers, G. Lajoinie, S. Cherkaoui, T. Bettinger, M. Versluis, M. Borden, Microbubble agents: new directions, Ultrasound Med. Biol. 46 (2020) 1326–1343.
[27] A. van Wamel, P.C. Sontum, A. Healey, S. Kvåle, N. Bush, J. Bamber, C.D.L. Davies, Acoustic Cluster Therapy (ACT) enhances the therapeutic efficacy of paclitaxel and Abraxane for treatment of human prostate adenocarcinoma in mice, J. Control. Release 236 (2016) 15–21.
[28] J.J. Kwan, R. Myers, C.M. Coviello, S.M. Graham, A.R. Shah, E. Stride, R.C. Carlisle, C.C. Coussios, Ultrasound-propelled nanocups for drug delivery, Small 11 (2015) 5305–5314.
[29] D.A. Fernandes, D.D. Fernandes, Y. Li, Y. Wang, Z. Zhang, D. Rousseau, C.C. Gradinaru, M.C. Kolios, Synthesis of stable multifunctional perfluorocarbon nanoemulsions for cancer therapy and imaging, Langmuir 32 (2016) 10870–10880.
[30] K. Yoo, W.R. Walker, R. Williams, C. Tremblay-Darveau, P.N. Burns, P.S. Sheeran, Impact of encapsulation on in vitro and in vivo performance of volatile nanoscale phase-shift perfluorocarbon droplets, Ultrasound Med. Biol. 44 (2018) 1836–1852.
[31] N. Rapoport, Drug-loaded perfluorocarbon nanodroplets for ultrasound-mediated drug delivery, Adv. Exp. Med. Biol. 880 (2016) 221–241.
[32] Ý. Mørch, R. Hansen, S. Berg, A.K.O. Åslund, W.R. Glomm, S. Eggen, R.B. Schmid, H. Johnsen, S. Kubowicz, S. Snipstad, E. Sulheim, S. Hak, G. Singh, B.H. McDonagh, H. Blom, C.d.L. Davies, P.M. Stenstad, Nanoparticle-stabilized microbubbles for multimodal imaging and drug delivery, Contrast Media Mol. Imaging 10 (2015) 356–366.
[33] C.W. Burke, E.t. Alexander, K. Timbie, A.L. Kilbanov, R.J. Price, Ultrasound-activated agents comprised of 5FU-bearing nanoparticles bonded to microbubbles inhibit solid tumor growth and improve survival, Mol. Ther. 22 (2014) 321–328.
[34] I. De Cock, G. Lajoinie, M. Versluis, S.C. De Smedt, I. Lentacker, Sonoprinting and the importance of microbubble loading for the ultrasound mediated cellular delivery of nanoparticles, Biomaterials 83 (2016) 294–307.
[35] Y.C. Chen, C.F. Chiang, S.K. Wu, L.F. Chen, W.Y. Hsieh, W.L. Lin, Targeting microbubbles-carrying TGFbeta1 inhibitor combined with ultrasound sonication induce BBB/BTB disruption to enhance nanomedicine treatment for brain tumors, J. Control. Release 211 (2015) 53–62.
[36] T. Segers, P. Kruizinga, M.P. Kok, G. Lajoinie, N. de Jong, M. Versluis, Monodisperse versus polydisperse ultrasound contrast agents: non-linear response, sensitivity, and deep tissue imaging potential, Ultrasound Med. Biol. 44 (2018) 1482–1492.
[37] B. van Elburg, G. Collado-Lara, G.W. Bruggert, T. Segers, M. Versluis, G. Lajoinie, Feedback-controlled microbubble generator producing one million monodisperse bubbles per second, Rev. Sci. Instrum. 92 (2021) 035110.
[38] J. Deprez, G. Lajoinie, Y. Engelen, S.C. De Smedt, I. Lentacker, Opening doors with ultrasound and microbubbles: Beating biological barriers to promote drug delivery, Adv. Drug Deliv. Rev. 172 (2021) 9–36.
[39] R.K. Jain, Determinants of tumor blood flow: a review, Cancer Res. 48 (1988) 2641–2658.
[40] J. Folkman, Tumor angiogenesis: therapeutic implications, N. Engl. J. Med. 285 (1971) 1182–1186.
[41] P. Carmeliet, R.K. Jain, Molecular mechanisms and clinical applications of angiogenesis, Nature 473 (2011) 298–307.
[42] Y. Wang, F. Yuan, Delivery of viral vectors to tumor cells: extracellular transport, systemic distribution, and strategies for improvement, Ann. Biomed. Eng. 34 (2006) 114–127.
[43] T.P. Padera, B.R. Stoll, J.B. Tooredman, D. Capen, E. di Tomaso, R.K. Jain, Pathology: cancer cells compress intratumour vessels, Nature 427 (2004) 695.

[44] A.K. Wood, R.M. Bunte, J.D. Cohen, J.H. Tsai, W.M. Lee, C.M. Sehgal, The antivascular action of physiotherapy ultrasound on a murine tumor: role of a microbubble contrast agent, Ultrasound Med. Biol. 33 (2007) 1901–1910.
[45] A.K. Wood, S. Ansaloni, L.S. Ziemer, W.M. Lee, M.D. Feldman, C.M. Sehgal, The antivascular action of physiotherapy ultrasound on murine tumors, Ultrasound Med. Biol. 31 (2005) 1403–1410.
[46] A.K. Wood, R.M. Bunte, H.E. Price, M.S. Deitz, J.H. Tsai, W.M. Lee, C.M. Sehgal, The disruption of murine tumor neovasculature by low-intensity ultrasound-comparison between 1- and 3-MHz sonication frequencies, Acad. Radiol. 15 (2008) 1133–1141.
[47] A.K. Wood, R.M. Bunte, S.M. Schultz, C.M. Sehgal, Acute increases in murine tumor echogenicity after antivascular ultrasound therapy: a pilot preclinical study, J. Ultrasound Med. 28 (2009) 795–800.
[48] A.K. Wood, S.M. Schultz, W.M. Lee, R.M. Bunte, C.M. Sehgal, Antivascular ultrasound therapy extends survival of mice with implanted melanomas, Ultrasound Med. Biol. 36 (2010) 853–857.
[49] D.E. Goertz, M. Todorova, O. Mortazavi, V. Agache, B. Chen, R. Karshafian, K. Hynynen, Antitumor effects of combining docetaxel (taxotere) with the antivascular action of ultrasound stimulated microbubbles, PLoS One 7 (2012) e52307.
[50] D.E. Goertz, R. Karshafian, K. Hynynen, Antivascular effects of pulsed low intensity ultrasound and microbubbles in mouse tumors, IEEE Ultrasonics Symposium (2008) 670–673.
[51] Goertz D.E., Karshafian R., Hynynen K., Investigating the effects of pulsed low intensity ultrasound and microbubbles in mouse tumors, in: IEEE International Ultrasonics Symposium Proceedings, 2009, pp. 89–92.
[52] Chin C.T., Raju B.I., Shevchenko T., Klibanov A.L., Control and reversal of tumor growth by ultrasound activated microbubbles, in: 2009 IEEE International Ultrasonics Symposium, 2009, pp. 77–80.
[53] C.W. Burke, A.L. Klibanov, J.P. Sheehan, R.J. Price, Inhibition of glioma growth by microbubble activation in a subcutaneous model using low duty cycle ultrasound without significant heating, J. Neurosurg. 114 (2011) 1654–1661.
[54] S.J. Hunt, T. Gade, M.C. Soulen, S. Pickup, C.M. Sehgal, Antivascular ultrasound therapy: magnetic resonance imaging validation and activation of the immune response in murine melanoma, J. Ultrasound Med. 34 (2015) 275–287.
[55] X. Hu, A. Kheirolomoom, L.M. Mahakian, J.R. Beegle, D.E. Kruse, K.S. Lam, K.W. Ferrara, Insonation of targeted microbubbles produces regions of reduced blood flow within tumor vasculature, Invest. Radiol. 47 (2012) 398–405.
[56] J.H. Hwang, A.A. Brayman, M.A. Reidy, T.J. Matula, M.B. Kimmey, L.A. Crum, Vascular effects induced by combined 1-MHz ultrasound and microbubble contrast agent treatments in vivo, Ultrasound Med. Biol. 31 (2005) 553–564.
[57] A. El Kaffas, M.J. Gangeh, G. Farhat, W.T. Tran, A. Hashim, A. Giles, G.J. Czarnota, Tumour vascular shutdown and cell death following ultrasound-microbubble enhanced radiation therapy, Theranostics 8 (2018) 314–327.
[58] A. Daecher, M. Stanczak, J.B. Liu, J. Zhang, S. Du, F. Forsberg, D.B. Leeper, J.R. Eisenbrey, Localized microbubble cavitation-based antivascular therapy for improving HCC treatment response to radiotherapy, Cancer Lett. 411 (2017) 100–105.
[59] P.T. Yemane, A.K.O. Aslund, S. Snipstad, A. Bjorkoy, K. Grendstad, S. Berg, Y. Morch, S.H. Torp, R. Hansen, C.L. Davies, Effect of ultrasound on the vasculature and extravasation of nanoscale particles imaged in real time, Ultrasound Med. Biol. 45 (2019) 3028–3041.
[60] M. Wu, Z. Song, S. Zhang, Q. Dan, C. Tang, C. Peng, Y. Liang, L. Zhang, H. Wang, Y. Li, Local tumor ischemia-reperfusion mediated by ultrasound-targeted microbubble destruction enhances the anti-tumor efficacy of doxorubicin chemotherapy, Cancer Manag. Res. 11 (2019) 9387–9395.
[61] J.T. Belcik, B.H. Mott, A. Xie, Y. Zhao, S. Kim, N.J. Lindner, A. Ammi, J.M. Linden, J.R. Lindner, Augmentation of limb perfusion and reversal of tissue ischemia produced by ultrasound-mediated microbubble cavitation, Circ. Cardiovasc. Imaging 8 (2015).
[62] S. Bertuglia, Increase in capillary perfusion following low-intensity ultrasound and microbubbles during postischemic reperfusion, Crit. Care Med. 33 (2005) 2061–2067.
[63] J.T. Belcik, B.P. Davidson, A. Xie, M.D. Wu, M. Yadava, Y. Qi, S. Liang, C.R. Chon, A.Y. Ammi, J. Field, L. Harmann, W.M. Chilian, J. Linden, J.R. Lindner, Augmentation of muscle blood flow by ultrasound cavitation is mediated by ATP and purinergic signaling, Circulation 135 (2017) 1240–1252.
[64] Y. Song, X. Xie, Y. Gao, L. Jin, P. Wang, Ultrasound-induced microbubble cavitation promotes angiogenesis in ischemic skeletal muscle of diabetic mice, Int. J. Clin. Exp. Med. 9 (2016) 23345–23350.
[65] A. Rix, M. Palmowski, F. Gremse, K. Palmowski, W. Lederle, F. Kiessling, J. Bzyl, Influence of repetitive contrast agent injections on functional and molecular ultrasound measurements, Ultrasound Med. Biol. 40 (2014) 2468–2475.
[66] Rix A., Flege B., Opacic T., Simons N., Koczera P., Kraus K., Stickeler E., Kiessling F., Contrast enhanced ultrasound treatment enhances tumor perfusion in breast cancer patients – first results, in: The 24th European symposium on Ultrasound Contrast Imaging, 2019.
[67] D.M. McDonald, P. Baluk, Significance of blood vessel leakiness in cancer, Cancer Res. 62 (2002) 5381–5385.
[68] D.M. McDonald, A.J. Foss, Endothelial cells of tumor vessels: abnormal but not absent, Cancer Metastasis Rev. 19 (2000) 109–120.
[69] S. Morikawa, P. Baluk, T. Kaidoh, A. Haskell, R.K. Jain, D.M. McDonald, Abnormalities in pericytes on blood vessels and endothelial sprouts in tumors, Am. J. Pathol. 160 (2002) 985–1000.
[70] H. Maeda, Toward a full understanding of the EPR effect in primary and metastatic tumors as well as issues related to its heterogeneity, Adv Drug Deliv Rev 91 (2015) 3–6.
[71] J. Park, Y. Choi, H. Chang, W. Um, J.H. Ryu, I.C. Kwon, Alliance with EPR effect: combined strategies to improve the EPR effect in the tumor microenvironment, Theranostics 9 (2019) 8073–8090.
[72] T. Lammers, F. Kiessling, W.E. Hennink, G. Storm, Drug targeting to tumors: principles, pitfalls and (pre-) clinical progress, J. Control. Release 161 (2012) 175–187.
[73] H. Maeda, Macromolecular therapeutics in cancer treatment: the EPR effect and beyond, J. Control. Release 164 (2012) 138–144.
[74] A.E. Hansen, A.L. Petersen, J.R. Henriksen, B. Boerresen, P. Rasmussen, D.R. Elema, P.M. Rosenschold, A.T. Kristensen, A. Kjaer, T.L. Andresen, Positron emission tomography based elucidation of the enhanced permeability and retention effect in dogs with cancer using copper-64 liposomes, ACS Nano 9 (2015) 6985–6995.
[75] K.J. Harrington, S. Mohammadtaghi, P.S. Uster, D. Glass, A.M. Peters, R.G. Vile, J.S. Stewart, Effective targeting of solid tumors in patients with locally advanced cancers by radiolabeled pegylated liposomes, Clin. Cancer Res. 7 (2001) 243–254.
[76] H. Lee, A.F. Shields, B.A. Siegel, K.D. Miller, I. Krop, C.X. Ma, P.M. LoRusso, P.N. Munster, K. Campbell, D.F. Gaddy, S.C. Leonard, E. Geretti, S.J. Blocker, D.B. Kirpotin, V. Moyo, T.J. Wickham, B.S. Hendriks, (64)Cu-MM-302 positron emission tomography quantifies variability of enhanced permeability and retention of nanoparticles in relation to treatment response in patients with metastatic breast cancer, Clin. Cancer Res. 23 (2017) 4190–4202.
[77] M.I. Koukourakis, S. Koukouraki, A. Giatromanolaki, S.C. Archimandritis, J. Skarlatos, K. Beroukas, J.G. Bizakis, G. Retalis, N. Karkavitsas, E.S. Helidonis, Liposomal doxorubicin and conventionally fractionated radiotherapy in the treatment of locally advanced non-small-cell lung cancer and head and neck cancer, J. Clin. Oncol. 17 (1999) 3512–3521.
[78] S. Patel, J. Kim, M. Herrera, A. Mukherjee, A.V. Kabanov, G. Sahay, Brief update on endocytosis of nanomedicines, Adv. Drug Deliv. Rev. 144 (2019) 90–111.
[79] M. Olsman, V. Sereti, K. Andreassen, S. Snipstad, A. van Wamel, R. Eliasen, S. Berg, A.J. Urquhart, T.L. Andresen, C.L. Davies, Ultrasound-mediated delivery enhances therapeutic efficacy of MMP sensitive liposomes, J. Control. Release 325 (2020) 121–134.
[80] B. Theek, M. Baues, T. Ojha, D. Mockel, S.K. Veettil, J. Steitz, L. van Bloois, G. Storm, F. Kiessling, T. Lammers, Sonoporation enhances liposome accumulation and penetration in tumors with low EPR, J. Control. Release 231 (2016) 77–85.
[81] T.Y. Wang, J.W. Choe, K.Y. Pu, R. Devulapally, S. Bachawal, S. Machtaler, S.M. Chowdhury, R. Luong, L. Tian, B. Khuri-Yakub, J.H. Rao, R. Paulmurugan, J.K. Willmann, Ultrasound-guided delivery of microRNA loaded nanoparticles into cancer, J. Control. Release 203 (2015) 99–108.
[82] A. Kheirolomoom, P.A. Dayton, A.F. Lum, E. Little, E.E. Paoli, H. Zheng, K.W. Ferrara, Acoustically-active microbubbles conjugated to liposomes: characterization of a proposed drug delivery vehicle, J. Control. Release 118 (2007) 275–284.
[83] F. Yan, L. Li, Z.T. Deng, Q.F. Jin, J.J. Chen, W. Yang, C.K. Yeh, J.R. Wu, R. Shandas, X. Liu, H.R. Zheng, Paclitaxel-liposome-microbubble complexes as ultrasound-triggered therapeutic drug delivery carriers, J. Control. Release 166 (2013) 246–255.
[84] P. Sontum, S. Kvale, A.J. Healey, R. Skurtveit, R. Watanabe, M. Matsumura, J. Ostensen, Acoustic Cluster Therapy (ACT)–A novel concept for ultrasound mediated, targeted drug delivery, Int. J. Pharm. 495 (2015) 1019–1027.
[85] A. van Wamel, A. Healey, P.C. Sontum, S. Kvale, N. Bush, J. Bamber, C.D.L. Davies, Acoustic Cluster Therapy (ACT) - pre-clinical proof of principle for local drug delivery and enhanced uptake, J. Control. Release 224 (2016) 158–164.
[86] M.R. Bohmer, C.H.T. Chlon, B.I. Raju, C.T. Chin, T. Shevchenko, A.L. Klibanov, Focused ultrasound and microbubbles for enhanced extravasation, J. Control. Release 148 (2010) 18–24.
[87] G. Wang, Z.X. Zhuo, H.M. Xia, Y. Zhang, Y. He, W.H. Tan, Y.H. Gao, Investigation into the impact of diagnostic ultrasound with microbubbles on the capillary permeability of rat hepatomas, Ultrasound Med. Biol. 39 (2013) 628–637.
[88] J.J. Choi, R.C. Carlisle, C. Coviello, L. Seymour, C.-C. Coussios, Non-invasive and real-time passive acoustic mapping of ultrasound-mediated drug delivery, Phys. Med. Biol. 59 (2014) 4861–4877.
[89] C.F. Caskey, S. Qin, P.A. Dayton, K.W. Ferrara, Microbubble tunneling in gel phantoms, J. Acoust. Soc. Am. 125 (2009) EL183–189.
[90] A. van Wamel, K. Kooiman, M. Harteveld, M. Emmer, F.J. ten Cate, M. Versluis, N. de Jong, Vibrating microbubbles poking individual cells: drug transfer into cells via sonoporation, J. Control. Release 112 (2006) 149–155.
[91] M. Afadzi, S.P. Strand, E.A. Nilssen, S.E. Måsøy, T.F. Johansen, R. Hansen, B.A. Angelsen, C.D.L. Davies, Mechanisms of the ultrasound-mediated intracellular delivery of liposomes and dextrans, IEEE Trans. Ultrason. Ferroelectr. Freq. Control 60 (2013) 21–33.
[92] B.D. Meijering, L.J. Juffermans, A. van Wamel, R.H. Henning, I.S. Zuhorn, M. Emmer, A.M. Versteilen, W.J. Paulus, W.H. van Gilst, K. Kooiman, N. de Jong, R. J. Musters, L.E. Deelman, O. Kamp, Ultrasound and microbubble-targeted delivery of macromolecules is regulated by induction of endocytosis and pore formation, Circ. Res. 104 (2009) 679–687.

[93] G. Lajoinie, I. De Cock, C.C. Coussios, I. Lentacker, S. Le Gac, E. Stride, M. Versluis, In vitro methods to study bubble-cell interactions: fundamentals and therapeutic applications, Biomicrofluidics 10 (2016) 011501.
[94] B. Helfield, X. Chen, S.C. Watkins, F.S. Villanueva, Biophysical insight into mechanisms of sonoporation, Proc. Natl. Acad. Sci. USA 113 (2016) 9983–9988.
[95] Y. Hu, J.M. Wan, A.C. Yu, Membrane perforation and recovery dynamics in microbubble-mediated sonoporation, Ultrasound Med. Biol. 39 (2013) 2393–2405.
[96] S. Bulner, A. Prodeus, J. Gariepy, K. Hynynen, D.E. Goertz, Enhancing checkpoint inhibitor therapy with ultrasound stimulated microbubbles, Ultrasound Med. Biol. 45 (2019) 500–512.
[97] H. Chen, W. Kreider, A.A. Brayman, M.R. Bailey, T.J. Matula, Blood vessel deformations on microsecond time scales by ultrasonic cavitation, Phys. Rev. Lett. 106 (2011) 034301.
[98] P.Y. Chen, H.Y. Hsieh, C.Y. Huang, C.Y. Lin, K.C. Wei, H.L. Liu, Focused ultrasound-induced blood-brain barrier opening to enhance interleukin-12 delivery for brain tumor immunotherapy: a preclinical feasibility study, J. Transl. Med. 13 (2015) 93.
[99] H.A. Hancock, L.H. Smith, J. Cuesta, A.K. Durrani, M. Angstadt, M.L. Palmeri, E. Kimmel, V. Frenkel, Investigations into pulsed high-intensity focused ultrasound-enhanced delivery: preliminary evidence for a novel mechanism, Ultrasound Med. Biol. 35 (2009) 1722–1736.
[100] C.P. Keravnou, I. De Cock, I. Lentacker, M.L. Izamis, M.A. Averkiou, Microvascular injury and perfusion changes induced by ultrasound and microbubbles in a machine-perfused pig liver, Ultrasound Med. Biol. 42 (2016) 2676–2686.
[101] S. Lee, H. Han, H. Koo, J.H. Na, H.Y. Yoon, K.E. Lee, H. Lee, H. Kim, I.C. Kwon, K. Kim, Extracellular matrix remodeling in vivo for enhancing tumor-targeting efficiency of nanoparticle drug carriers using the pulsed high intensity focused ultrasound, J. Control. Release 263 (2017) 68–78.
[102] T. Li, Y.N. Wang, T.D. Khokhlova, S. D'Andrea, F. Starr, H. Chen, J.S. McCune, L.J. Risler, A. Mashadi-Hossein, S.R. Hingorani, A. Chang, J.H. Hwang, Pulsed high-intensity focused ultrasound enhances delivery of doxorubicin in a preclinical model of pancreatic cancer, Cancer Res. 75 (2015) 3738–3746.
[103] H.L. Liu, H.Y. Hsieh, L.A. Lu, C.W. Kang, M.F. Wu, C.Y. Lin, Low-pressure pulsed focused ultrasound with microbubbles promotes an anticancer immunological response, J. Transl. Med. 10 (2012) 221.
[104] J. Sekino, M. Nagao, S. Kato, M. Sakai, K. Abe, E. Nakayama, M. Sato, Y. Nagashima, H. Hino, N. Tanabe, T. Kawato, M. Maeno, N. Suzuki, K. Ueda, Low-intensity pulsed ultrasound induces cartilage matrix synthesis and reduced MMP13 expression in chondrocytes, Biochem. Biophys. Res. Commun. 506 (2018) 290–297.
[105] Y. Song, X. Xie, Y. Gao, G. Gu, P. Wang, Ultrasound-induced microbubble destruction promotes targeted delivery of adipose-derived stem cells to improve hind-limb ischemia of diabetic mice, Am. J. Transl. Res. 8 (2016) 2585–2596.
[106] W.L. Suen, J. Jiang, H.S. Wong, J. Qu, Y. Chau, Examination of effects of low-frequency ultrasound on scleral permeability and collagen network, Ultrasound Med. Biol. 42 (2016) 2650–2661.
[107] R. Suzuki, E. Namai, Y. Oda, N. Nishiie, S. Otake, R. Koshima, K. Hirata, Y. Taira, N. Utoguchi, Y. Negishi, S. Nakagawa, K. Maruyama, Cancer gene therapy by IL-12 gene delivery using liposomal bubbles and tumoral ultrasound exposure, J. Control. Release 142 (2010) 245–250.
[108] K.D. Watson, C.Y. Lai, S. Qin, D.E. Kruse, Y.C. Lin, J.W. Seo, R.D. Cardiff, L.M. Mahakian, J. Beegle, E.S. Inghanm, F.R. Curry, R.K. Reed, K.W. Ferrara, Ultrasound increases nanoparticle delivery by reducing intratumoral pressure and increasing transport in epithelial and epithelial-mesenchymal transition tumors, Cancer Res. 72 (2012) 1485–1493.
[109] J.C. Wischhusen, S.M. Chowdhury, T. Lee, H. Wang, S. Bachawal, R. Devulapally, R. Afjei, U.K. Sukumar, R. Paulmurugan, Ultrasound-mediated delivery of miRNA-122 and anti-miRNA-21 therapeutically immunomodulates murine hepatocellular carcinoma in vivo, J. Control. Release 321 (2020) 272–284.
[110] N. Xiao, J. Liu, L. Liao, J. Sun, W. Jin, X. Shu, Ultrasound combined with microbubbles increase the delivery of doxorubicin by reducing the interstitial fluid pressure, Ultrasound Q 35 (2019) 103–109.
[111] C. Yang, M. Du, F. Yan, Z. Chen, Focused ultrasound improves NK-92MI cells infiltration into tumors, Front. Pharmacol. 10 (2019) 326.
[112] Q. Zhang, H. Jin, L. Chen, Q. Chen, Y. He, Y. Yang, S. Ma, S. Xiao, F. Xi, Q. Luo, J. Liu, Effect of ultrasound combined with microbubble therapy on interstitial fluid pressure and VX2 tumor structure in rabbit, Front. Pharmacol. 10 (2019) 716.
[113] O. Zolochevska, X. Xia, B.J. Williams, A. Ramsay, S. Li, M.L. Figueiredo, Sonoporation delivery of interleukin-27 gene therapy efficiently reduces prostate tumor cell growth in vivo, Hum. Gene Ther. 22 (2011) 1537–1550.
[114] E. Henke, R. Nandigama, S. Ergun, Extracellular matrix in the tumor microenvironment and its impact on cancer therapy, Front. Mol. Biosci. 6 (2019) 160.
[115] J.L. Au, B.Z. Yeung, M.G. Wientjes, Z. Lu, M.G. Wientjes, Delivery of cancer therapeutics to extracellular and intracellular targets: determinants, barriers, challenges and opportunities, Adv. Drug Deliv. Rev. 97 (2016) 280–301.
[116] P. Tharkar, R. Varanasi, W.S.F. Wong, C.T. Jin, W. Chrzanowski, Nano-enhanced drug delivery and therapeutic ultrasound for cancer treatment and beyond, Front. Bioeng. Biotechnol. 7 (2019) 324.
[117] S. Nallanthighal, J.P. Heiserman, D.J. Cheon, The role of the extracellular matrix in cancer stemness, Front. Cell Dev. Biol. 7 (2019) 86.
[118] E.G. Canty, K.E. Kadler, Procollagen trafficking, processing and fibrillogenesis, J. Cell Sci. 118 (2005) 1341–1353.
[119] P.P. Provenzano, K.W. Eliceiri, J.M. Campbell, D.R. Inman, J.G. White, P.J. Keely, Collagen reorganization at the tumor-stromal interface facilitates local invasion, BMC Med. 4 (2006) 38.
[120] N.I. Nissen, M. Karsdal, N. Willumsen, Collagens and cancer associated fibroblasts in the reactive stroma and its relation to Cancer biology, J. Exp. Clin. Cancer Res. 38 (2019) 115.
[121] T. Stylianopoulos, J.D. Martin, V.P. Chauhan, S.R. Jain, B. Diop-Frimpong, N. Bardeesy, B.L. Smith, C.R. Ferrone, F.J. Hornicek, Y. Boucher, L.L. Munn, R.K. Jain, Causes, consequences, and remedies for growth-induced solid stress in murine and human tumors, Proc. Natl. Acad. Sci. USA 109 (2012) 15101–15108.
[122] C. Voutouri, T. Stylianopoulos, Accumulation of mechanical forces in tumors is related to hyaluronan content and tissue stiffness, PLoS One 13 (2018) e0193801.
[123] P.A. Netti, D.A. Berk, M.A. Swartz, A.J. Grodzinsky, R.K. Jain, Role of extracellular matrix assembly in interstitial transport in solid tumors, Cancer Res. 60 (2000) 2497–2503.
[124] E.A. Swabb, J. Wei, P.M. Gullino, Diffusion and convection in normal and neoplastic tissues, Cancer Res. 34 (1974) 2814–2822.
[125] T. Liu, L. Zhou, D. Li, T. Andl, Y. Zhang, Cancer-associated fibroblasts build and secure the tumor microenvironment, Front. Cell Dev. Biol. 7 (2019) 60.
[126] R. Pidsley, M.G. Lawrence, E. Zotenko, B. Niranjan, A. Statham, J. Song, R.M. Chabanon, W. Qu, H. Wang, M. Richards, S.S. Nair, N.J. Armstrong, H.T. Nim, M. Papargiris, P. Balanathan, H. French, T. Peters, S. Norden, A. Ryan, J. Pedersen, J. Kench, R.J. Daly, L.G. Horvath, P. Stricker, M. Frydenberg, R.A. Taylor, C. Stirzaker, G.P. Risbridger, S.J. Clark, Enduring epigenetic landmarks define the cancer microenvironment, Genome Res. 28 (2018) 625–638.
[127] Y. Che, J. Wang, Y. Li, Z. Lu, J. Huang, S. Sun, S. Mao, Y. Lei, R. Zang, N. Sun, J. He, Cisplatin-activated PAI-1 secretion in the cancer-associated fibroblasts with paracrine effects promoting esophageal squamous cell carcinoma progression and causing chemoresistance, Cell Death Dis. 9 (2018) 759.
[128] Y. Mao, E.T. Keller, D.H. Garfield, K. Shen, J. Wang, Stromal cells in tumor microenvironment and breast cancer, Cancer Metastasis Rev. 32 (2013) 303–315.
[129] I.A. Khawar, J.H. Kim, H.J. Kuh, Improving drug delivery to solid tumors: priming the tumor microenvironment, J. Control. Release 201 (2015) 78–89.
[130] E.L. Siegler, Y.J. Kim, P. Wang, Nanomedicine targeting the tumor microenvironment: therapeutic strategies to inhibit angiogenesis, remodel matrix, and modulate immune responses, J. Cell. Immunother. 2 (2016) 69–78.
[131] Y. Omidi, J. Barar, Targeting tumor microenvironment: crossing tumor interstitial fluid by multifunctional nanomedicines, Bioimpacts 4 (2014) 55–67.
[132] R.K. Jain, Normalization of tumor vasculature: an emerging concept in antiangiogenic therapy, Science 307 (2005) 58–62.
[133] T. Stylianopoulos, J.D. Martin, M. Snuderl, F. Mpekris, S.R. Jain, R.K. Jain, Coevolution of solid stress and interstitial fluid pressure in tumors during progression: implications for vascular collapse, Cancer Res. 73 (2013) 3833–3841.
[134] M. Kalli, T. Stylianopoulos, Defining the role of solid stress and matrix stiffness in cancer cell proliferation and metastasis, Front. Oncol. 8 (2018) 55.
[135] V. Gkretsi, T. Stylianopoulos, Cell adhesion and matrix stiffness: coordinating cancer cell invasion and metastasis, Front. Oncol. 8 (2018) 145.
[136] H.T. Nia, M. Datta, G. Seano, P. Huang, L.L. Munn, R.K. Jain, Quantifying solid stress and elastic energy from excised or in situ tumors, Nat. Protoc. 13 (2018) 1091–1105.
[137] J.M. Northcott, I.S. Dean, J.K. Mouw, V.M. Weaver, Feeling stress: the mechanics of cancer progression and aggression, Front. Cell Dev. Biol. 6 (2018) 17.
[138] T. Stylianopoulos, L.L. Munn, R.K. Jain, Reengineering the physical microenvironment of tumors to improve drug delivery and efficacy: from mathematical modeling to bench to bedside, Trends Cancer 4 (2018) 292–319.
[139] G. Kharaishvili, D. Simkova, K. Bouchalova, M. Gachechiladze, N. Narsia, J. Bouchal, The role of cancer-associated fibroblasts, solid stress and other microenvironmental factors in tumor progression and therapy resistance, Cancer Cell Int. 14 (2014) 41.
[140] Y. Boucher, R.K. Jain, Microvascular pressure is the principal driving force for interstitial hypertension in solid tumors - implications for vascular collapse, Cancer Res. 52 (1992) 5110–5114.
[141] G. Vlahovic, A.M. Ponce, Z. Rabbani, F.K. Salahuddin, L. Zgonjanin, I. Spasojevic, Z. Vujaskovic, M.W. Dewhirst, Treatment with imatinib improves drug delivery and efficacy in NSCLC xenografts, Br. J. Cancer 97 (2007) 735–740.
[142] K. Pietras, K. Rubin, T. Sjoblom, E. Buchdunger, M. Sjoquist, C.H. Heldin, A. Ostman, Inhibition of PDGF receptor signaling in tumor stroma enhances antitumor effect of chemotherapy, Cancer Res. 62 (2002) 5476–5484.
[143] V.P. Chauhan, J.D. Martin, H. Liu, D.A. Lacorre, S.R. Jain, S.V. Kozin, T. Stylianopoulos, A.S. Mousa, X. Han, P. Adstamongkonkul, Z. Popovic, P. Huang, M.G. Bawendi, Y. Boucher, R.K. Jain, Angiotensin inhibition enhances drug delivery and potentiates chemotherapy by decompressing tumour blood vessels, Nat. Commun. 4 (2013) 2516.
[144] A. Dolor, F.C. Szoka Jr., Digesting a path forward: the utility of collagenase tumor treatment for improved drug delivery, Mol. Pharm. 15 (2018) 2069–2083.

[145] C. Brekken, O.S. Bruland, C. de Lange Davies, Interstitial fluid pressure in human osteosarcoma xenografts: significance of implantation site and the response to intratumoral injection of hyaluronidase, Anticancer Res. 20 (2000) 3503–3512.
[146] P. Hadaczek, Y. Yamashita, H. Mirek, L. Tamas, M.C. Bohn, C. Noble, J.W. Park, K. Bankiewicz, The "perivascular pump" driven by arterial pulsation is a powerful mechanism for the distribution of therapeutic molecules within the brain, Mol. Ther. 14 (2006) 69–78.
[147] L. Eikenes, M. Tari, I. Tufto, O.S. Bruland, C.D. Davies, Hyaluronidase induces a transcapillary pressure gradient and improves the distribution and uptake of liposomal doxorubicin (Caelyx (TM)) in human osteosarcoma xenografts, Br. J. Cancer 93 (2005) 81–88.
[148] M.D. Nieskoski, K. Marra, J.R. Gunn, S.C. Kanick, M.M. Doyley, T. Hasan, S.P. Pereira, B. Stuart Trembly, B.W. Pogue, Separation of solid stress from interstitial fluid pressure in pancreas cancer correlates with collagen area fraction, J. Biomech. Eng. 139 (2017).
[149] D. Hanahan, R.A. Weinberg, Hallmarks of cancer: the next generation, Cell 144 (2011) 646–674.
[150] E.C. Finger, A.J. Giaccia, Hypoxia, inflammation, and the tumor microenvironment in metastatic disease, Cancer Metastasis Rev. 29 (2010) 285–293.
[151] Q. Dai, S. Wilhelm, D. Ding, A.M. Syed, S. Sindhwani, Y. Zhang, Y.Y. Chen, P. MacMillan, W.C.W. Chan, Quantifying the ligand-coated nanoparticle delivery to cancer cells in solid tumors, ACS Nano 12 (2018) 8423–8435.
[152] M.A. Miller, Y.R. Zheng, S. Gadde, C. Pfirschke, H. Zope, C. Engblom, R.H. Kohler, Y. Iwamoto, K.S. Yang, B. Askevold, N. Kolishetti, M. Pittet, S.J. Lippard, O.C. Farokhzad, R. Weissleder, Tumour-associated macrophages act as a slow-release reservoir of nano-therapeutic Pt(IV) pro-drug, Nat. Commun. 6 (2015) 8692.
[153] Y.J. Ho, J.P. Li, C.H. Fan, H.L. Liu, C.K. Yeh, Ultrasound in tumor immunotherapy: current status and future developments, J. Control. Release 323 (2020) 12–23.
[154] J. Unga, M. Hashida, Ultrasound induced cancer immunotherapy, Adv. Drug Deliv. Rev. 72 (2014) 144–153.
[155] Z.I. Kovacs, S. Kim, N. Jikaria, F. Qureshi, B. Milo, B.K. Lewis, M. Bresler, S.R. Burks, J.A. Frank, Disrupting the blood-brain barrier by focused ultrasound induces sterile inflammation, Proc. Natl. Acad. Sci. USA 114 (2017) E75–E84.
[156] R. Alkins, A. Burgess, R. Kerbel, W.S. Wels, K. Hynynen, Early treatment of HER2-amplified brain tumors with targeted NK-92 cells and focused ultrasound improves survival, Neuro Oncol. 18 (2016) 974–981.
[157] R. Alkins, A. Burgess, M. Ganguly, G. Francia, R. Kerbel, W.S. Wels, K. Hynynen, Focused ultrasound delivers targeted immune cells to metastatic brain tumors, Cancer Res. 73 (2013) 1892–1899.
[158] K. Anwer, C. Meaney, G. Kao, N. Hussain, R. Shelvin, R.M. Earls, P. Leonard, A. Quezada, A.P. Rolland, S.M. Sullivan, Cationic lipid-based delivery system for systemic cancer gene therapy, Cancer Gene Ther. 7 (2000) 1156–1164.
[159] E. Daguenet, S. Louati, A.S. Wozny, N. Vial, M. Gras, J.B. Guy, A. Vallard, C. Rodriguez-Lafrasse, N. Magne, Radiation-induced bystander and abscopal effects: important lessons from preclinical models, Br. J. Cancer 123 (2020) 339–348.
[160] P. Lai, C. Tarapacki, W.T. Tran, A. El Kaffas, J. Lee, C. Hupple, S. Iradji, A. Giles, A. Al-Mahrouki, G.J. Czarnota, Breast tumor response to ultrasound mediated excitation of microbubbles and radiation therapy in vivo, Oncoscience 3 (2016) 98–108.
[161] A.K.O. Åslund, S. Berg, S. Hak, Ý. Mørch, S.H. Torp, A. Sandvig, M. Widerøe, R. Hansen, C.D.L. Davies, Nanoparticle delivery to the brain–By focused ultrasound and self-assembled nanoparticle-stabilized microbubbles, J. Control. Release 220 (2015) 287–294.
[162] A. Burgess, C.A. Ayala-Grosso, M. Ganguly, J.F. Jordao, I. Aubert, K. Hynynen, Targeted delivery of neural stem cells to the brain using MRI-guided focused ultrasound to disrupt the blood-brain barrier, PLoS One 6 (2011) e27877.
[163] C. Poon, D. McMahon, K. Hynynen, Noninvasive and targeted delivery of therapeutics to the brain using focused ultrasound, Neuropharmacology (2016).
[164] T. Kobus, I.K. Zervantonakis, Y. Zhang, N.J. McDannold, Growth inhibition in a brain metastasis model by antibody delivery using focused ultrasound-mediated blood-brain barrier disruption, J. Control. Release 238 (2016) 281–288.
[165] A.B. Etame, R.J. Diaz, M.A. O'Reilly, C.A. Smith, T.G. Mainprize, K. Hynynen, J.T. Rutka, Enhanced delivery of gold nanoparticles with therapeutic potential into the brain using MRI-guided focused ultrasound, Nanomed.-Nanotechnol. 8 (2012) 1133–1142.
[166] A. Carpentier, M. Canney, A. Vignot, V. Reina, K. Beccaria, C. Horodyckid, C. Karachi, D. Leclercq, C. Lafon, J.Y. Chapelon, L. Capelle, P. Cornu, M. Sanson, K. Hoang-Xuan, J.Y. Delattre, A. Idbaih, Clinical trial of blood-brain barrier disruption by pulsed ultrasound, Sci. Transl. Med. 8 (2016) 343re342.
[167] T. Mainprize, N. Lipsman, Y. Huang, Y. Meng, A. Bethune, S. Ironside, C. Heyn, R. Alkins, M. Trudeau, A. Sahgal, J. Perry, K. Hynynen, Blood-brain barrier opening in primary brain tumors with non-invasive MR-guided focused ultrasound: a clinical safety and feasibility study, Sci. Rep. 9 (2019) 321.
[168] A. Idbaih, M. Canney, L. Belin, C. Desseaux, A. Vignot, G. Bouchoux, N. Asquier, B. Law-Ye, D. Leclercq, A. Bissery, Y. De Rycke, C. Trosch, L. Capelle, M. Sanson, K. Hoang-Xuan, C. Dehais, C. Houillier, F. Laigle-Donadey, B. Mathon, A. Andre, C. Lafon, J.Y. Chapelon, J.Y. Delattre, A. Carpentier, Safety and feasibility of repeated and transient blood-brain barrier disruption by pulsed ultrasound in patients with recurrent glioblastoma, Clin. Cancer Res. 25 (2019) 3793–3801.
[169] M.D. McSweeney, Z.C. Versfeld, D.M. Carpenter, S.K. Lai, Physician awareness of immune responses to polyethylene glycol-drug conjugates, Clin. Transl. Sci. 11 (2018) 162–165.
[170] S. Roovers, T. Segers, G. Lajoinie, J. Deprez, M. Versluis, S.C. De Smedt, I. Lentacker, The role of ultrasound-driven microbubble dynamics in drug delivery: from microbubble fundamentals to clinical translation, Langmuir 35 (2019) 10173–10191.
[171] A.A. Doinikov, J.F. Haac, P.A. Dayton, Resonance frequencies of lipid-shelled microbubbles in the regime of nonlinear oscillations, Ultrasonics 49 (2009) 263–268.
[172] F.T. Dastous, F.S. Foster, Frequency-dependence of ultrasound attenuation and backscatter in breast-tissue, Ultrasound Med. Biol. 12 (1986) 795–808.
[173] Y.R. Zhang, R. Lin, H.J. Li, W.L. He, J.Z. Du, J. Wang, Strategies to improve tumor penetration of nanomedicines through nanoparticle design, Wires Nanomed. Nanobi. 11 (2019).